Statistical mechanics of the 3D axisymmetric Euler equations in a Taylor-Couette geometry

Simon Thalabard, Bérengère Dubrulle, Freddy Bouchet

Statistical mechanics of the 3D axisymmetric Euler equations in a Taylor-Couette geometry

Simon Thalabard[1] *, Bérengère Dubrulle[1] and Freddy Bouchet[2]

[1] *Laboratoire SPHYNX, Service de Physique de l'Etat Condensé, DSM, CEA Saclay, CNRS URA 2464, 91191 Gif-sur-Yvette, France*
[2] *Laboratoire de Physique de l'Ecole Normale Supérieure de Lyon, Université de Lyon and CNRS, 46, Allée d'Italie, F-69007 Lyon, France*

June 5, 2013

Abstract

Using an analogy with an Ising-like spin model, we define microcanonical measures for the dynamics of three dimensional (3D) axisymmetric turbulent flow in a Taylor-Couette geometry. We compute the relevant physical quantities and argue that axisymmetry induces a large scale organization in turbulent flows. We show that there exists a low energy, low temperature regime, for which the orthoradial velocity field is organized into vertical stripes, as well as a high energy, infinite temperature regime where the typical orthoradial vorticity field gets organized into either a single vertical jet or a large scale dipole, and exhibits infinite fluctuations. The mechanisms yielding the large scale organizations are argued to be different from the ones involved in two dimensional (2D) turbulence. This shows that the 3D axisymmetric case is truly an intermediate case between 2D and 3D turbulence.

Contents

*simon.thalabard@cea.fr

1 Introduction

Statistical mechanics provided powerful tools to study complex dynamical systems in all fields of physics. However, it proved extremely difficult to apply classical statistical mechanics ideas to turbulence problems. The main reason is that many statistical mechanics theories relie on equilibrium or close to equilibrium results, based on the microcanonical measures. Yet, one of the main phenomena of classical three dimensional (3D) turbulence is the anomalous dissipation, namely the existence of an energy flux towards small scales that remains finite in the inertial limit of an infinite Reynolds number. This makes the classical 3D turbulence problem an intrinsic non-equilibrium problem. Hence, microcanonical measures have long been thought to be irrelevant for turbulence problems.

A purely equilibrium statistical mechanics approach to 3D turbulence is actually pathological. Indeed, it leads for any finite dimensional approximation to an equipartition spectrum, which has no well defined asymptotic behavior in the limit of an infinite number of degrees of freedom [Bouchet and Venaille, 2011]. This phenomena, related to the Rayleigh-Jeans paradox of the equilibrium statistical mechanics of classical fields [Pomeau, 1994], is a sign that an equilibrium approach is bound to fail. This is consistent with the observed phenomena of anomalous dissipation for the 3D Navier-Stokes and suspected equivalent anomalous dissipation phenomena for the 3D Euler equations.

The case of the 2D Euler equations and related Quasi-Geostrophic dynamics is a remarkable exception to the rule that equilibrium statistical mechanics fails for classical field theories. In this case, the existence of a new class of invariants (Casimirs), among them enstrophy, leads to a completely different picture. Onsager first anticipated this difference when he studied the statistical mechanics of the point vortex model, which is a

class of special solutions to the 2D Euler equations [Onsager, 1949,Eyink and Sreenivasan, 2006]. After the initial works of Robert, Sommeria and Miller in the nineties [Miller, 1990, Robert and Sommeria, 1991, Robert and Sommeria, 1992] and subsequent work [Michel and Robert, 1994, Jordan and Turkington, 1997, Ellis et al., 2004, Majda and Wang, 2006, Bouchet and Corvellec, 2010], it is now clear that microcanonical measures taking into account all invariants exist for the 2D Euler equations. These microcanonical measures can be built through finite dimensional approximations. The finite dimensional approximate measure has then a well defined limit, which verifies some large deviations properties (see for instance [Potters et al., 2013] for a recent simple discussion of this construction). The physics described by this statistical mechanics approach is a self-organization of the flow into a large scale coherent structure corresponding to the most probable macrostate.

The three dimensional axisymmetric Euler equations describe the motion of a perfect three dimensional flow, assumed to be symmetric with respect to rotations around a fixed axis. Such flows have additional Casimir invariants (toroidal Casimirs and generalized Helicities, defined below). By contrast with the 2D Euler equations, it has yet never been proven that Casimir constraints should prevent an energy cascade towards smaller and smaller scales, although it has been stated that the dynamics of such flows will lead to predictable large scale structures [Monchaux et al., 2006]. Based on these remarks, the three dimensional axisymmetric Euler equations seem to be an intermediate case between 2D and 3D Euler equations, as previously suggested in [Leprovost et al., 2006, Naso et al., 2010a]. It is then extremely natural to address the issue of the existence or not of non-trivial microcanonical measures.

In this paper we define approximate microcanonical measures on spaces of finite dimensional approximations of axisymmetric flows, compatible with a formal Liouville theorem. As the constrained invariant subspace of the phase space is not bounded, we also have to consider an artificial cutoff M on the accessible vorticity values. From these approximate microcanonical measures, we compute the probability distribution of poloidal and toroidal part of the velocity field. The microcanonical measure of the 3D axisymmetric equations is defined as a weak limit of sequences of those finite dimensional approximate microcanonical measures, when the cutoff M goes to infinity. More heuristically stated, we will show that finite dimensional approximations of the Euler equations can be mapped onto an Ising-like model whose thermodynamic limit corresponds to a microcanonical measure of the Euler equations. We prove that this limit exists and that it describes non-trivial flow structures.

The main physical result is the existence of two kinds of statistical equilibria, depending on the values of the energy. Low energy equilibria are caracterized by a positive microcanonical temperature and describe large scale toroidal coherent structures with a vanishing poloidal field. High energy equilibria are caracterized by an infinite microcanonical temperature. Those equilibria correspond to a uniform and completely intertwined toroidal field. The typical poloidal field is dominated by large scales and exhibits infinitely large fluctuations.

Prior to the present work, Leprovost, Chavanis and Dubrulle [Leprovost et al., 2006, Naso et al., 2010a] attempted to describe statistical equilibria of the 3D axisymmetric equations. These previous works where not building microcanonical measure theoretically from the Liouville theorem, but were rather treating the toroidal part of the hydrodynamical field by analogy with the statistical mechanics of the 2D Euler equation, and

neglecting the effect of possible poloidal fluctuations. Wether such an approach should lead to invariant measures of the axisymmetric 3D Euler equation is not clear. We note that with our more natural approach, we obtain the same results as Leprovost, Chavanis and Dubrulle in the limit when the cutoff M goes to zero, whereas the actual microcanonical measures are obtained in the limit $M \to \infty$.

A very interesting question is the interest of the microcanonical measure for experimental 3D flows in an axisymmetric geometry. This issue is extremely subtle, and we postpone the discussion to brief comments in the conclusion and to a forthcoming paper.

In Section 2 we introduce the axisymmetric Euler equations together with their associated Casimir functions. We then relate the axisymmetric statistical equilibria to the asymptotic equilibria of an Ising-like spin model. In Section 3 we compute and describe the equilibria in the simplified case where the correlations between the toroidal and the poloidal fields are ignored. Those correlations are restored in Section 4. We discuss the main physical results and comment on the case $M = 0$ in section 5.

2 Mapping the axisymmetric Euler equations onto a spin model

In this section, we introduce the axisymmetric Euler equations and their invariants. We discretize them and observe that the corresponding equilibrium statistical model is equivalent to an Ising like spin model with non local interactions. We argue that the microcanonical thermodynamic limit of the spin model, corresponding to the continuous limit of the fluid mechanics model induces an invariant measure of the axisymmetric Euler equations.

2.1 Axisymmetric Euler equations and dynamical invariants

2.1.1 Equations

The starting point of the study are the Euler equations for incompressible flows inside a domain $\mathcal{D}$ made of two concentric cylindric walls of height $2h$, with internal radius R_{in} and outer one R_{out}. Those equations read

$$\partial_t \mathbf{v} + \mathbf{v}.\nabla\mathbf{v} = -\nabla\mathbf{p} \quad \text{and} \quad \nabla.\mathbf{v} = \mathbf{0}. \tag{1}$$

We use cylindrical coordinates (r, θ, z) and consider axisymmetric flows with a cylindrical geometry. They are defined through the three velocity components v_r, v_θ and v_z depending on r and z only. Instead of the usual velocity variables $\mathbf{v}$, it is convenient to write the Euler equations for axisymmetric flows in terms of a toroidal field $\sigma = r v_\theta$, together with a poloidal field $\xi = \dfrac{\omega_\theta}{r} = \dfrac{\partial_z v_r - \partial_r v_z}{r}$. It is also more convenient to use the coordinate $y = \dfrac{r^2}{2}$ instead of r, and we write $\mathbf{dx} = \mathrm{d}y\mathrm{d}\theta\mathrm{d}z$ the infinitesimal cylindrical volume element at position $(\mathbf{x}) = (y, \theta, z)$.

In the present study, we focus on velocity fields which are $2h$-periodic along the vertical direction and which satisfy an impermeability boundary condition on the two cylindric walls. Because the flow is incompressible ($\nabla.\mathbf{v} = 0$), we know (Helmholtz decomposition) that there exists a periodic stream function ψ and a constant C such that

$(2y)^{\frac{1}{2}} v_r = -\partial_z \psi + C$ and $v_z = \partial_y \psi$. The stream function is unique up to an additive constant. The impermeability boundary condition $\mathbf{v}.\mathbf{n}|_{\partial\mathcal{D}} = 0$ – with $\mathbf{n}$ the unit vector normal to the boundary $\partial\mathcal{D}$ – imposes that $C = 0$, ψ is constant on the outer wall and on the inner wall. Because ψ is defined up to a constant, the first constant can be chosen equal to zero without lack of generality. We note that $\psi|_{R_{in}^2/2} - \psi|_{R_{out}^2/2} = (2h)^{-1} \int \mathrm{d}y\mathrm{d}z \partial_y \psi = (2h)^{-1} \int \mathrm{d}y\mathrm{d}z v_z = \mathcal{M}_z$. The velocity field is z-periodic so the quantity $\mathcal{M}_z$ is a constant of motion. Therefore, we can choose to consider the referential for which this constant is zero and thus $\psi|_{R_{in}^2/2} = \psi|_{R_{out}^2/2} = 0$.

The fields ξ and ψ are related through

$$-\xi = \Delta^\star \psi = \frac{1}{2y}\partial_{zz}\psi + \partial_{yy}\psi, \quad \text{and} \quad \psi = 0 \ \text{ on both the inner and the outer walls.} \tag{2}$$

There is thus a one to one relation between (σ, ξ) and the incompressibility relation on one hand, and the velocity field on the other hand.

The axisymmetric Euler equations for the (σ, ξ) variables read [Leprovost et al., 2006]

$$\partial_t \sigma + \{\sigma, \psi\} = 0 \quad \text{and} \quad \partial_t \xi + \{\xi, \psi\} = \partial_z \frac{\sigma^2}{4y}. \tag{3}$$

The inner-brackets represent the advection terms and are defined by $\{f, g\} = \partial_y f \partial_z g - \partial_z f \partial_y g$.

Unless stated otherwise we will assume from now on that R_{in} is non-zero ($R_{in} > 0$). We denote $|\mathcal{D}| = 2h\pi \left(R_{out}^2 - R_{in}^2\right)$ the volume of the domain $\mathcal{D}$.

2.1.2 Dynamical invariants

It is straightforward to check that the kinetic energy $E = \frac{1}{2}\int_{\mathcal{D}} \mathbf{dx}\, \mathbf{v}^2$ is a conserved quantity of the axisymmetric Euler equations (3). The kinetic energy can be written in terms of the fields σ and ξ as

$$E = \frac{1}{2}\int_{\mathcal{D}} \mathbf{dx} \left[\frac{\sigma^2}{2y} + \xi\psi\right]. \tag{4}$$

As a consequence of Noether's theorem (for the relabelling symmetry) and the degeneracy of its Hamiltonian structure ([Morrison, 1998, Szeri and Holmes, 1988]), the axisymmetric Euler equations have infinitely many Casimir invariants. They fall into two families: the toroidal Casimirs C_f and the generalized Helicities H_g, defined by

$$C_f = \int_{\mathcal{D}} \mathbf{dx}\, f(\sigma) \quad \text{and} \quad H_g = \int_{\mathcal{D}} \mathbf{dx}\, \xi g(\sigma), \tag{5}$$

where f and g can be any sufficiently regular functions.

Note that the well-known invariants of the incompressible Euler equations correspond to specific choices for the functions f and g. The conservation of the usual helicity $H = \int_{\mathcal{D}} \mathbf{dx}\, \mathbf{v}.\omega$ is for instance recovered by setting $g(x) \equiv 2x$ in equation (5). Setting $f(x) \equiv x$ gives the conservation of the z-component of the angular momentum. Setting $g(x) \equiv 1$ gives the conservation of the circulation of the velocity field along a closed loop following the boundary of a meridional plane.

2.2 Dynamical invariants seen as geometrical constraints

We can give an alternative, more geometric, description of the Casimirs constraints (5). We introduce the indicator function $\mathbf{1}_{B(x)}$. This function takes value 1 if $B(x)$ is true and 0 otherwise. Now, given a value q for the toroidal field, let us set $f \equiv g \equiv \mathbf{1}_{\sigma(\mathbf{x})\leq q}$ in equation (5). Doing so, we obtain the specific toroidal Casimirs $\mathcal{C}_q(\sigma) = \int_{\mathcal{D}} \mathbf{dx}\, \mathbf{1}_{\sigma(\mathbf{x})\leq q}$ together whith the specific generalized Helicities $\mathcal{H}_q(\sigma,\xi) = \int_{\mathcal{D}} \mathbf{dx}\, \xi\,(\mathbf{x})\, \mathbf{1}_{\sigma(\mathbf{x})\leq q}$.

$\mathcal{C}_q$ represents the area of $\mathcal{D}$ where the toroidal field is lower than a prescribed value q. $\mathcal{H}_q$ can be interpreted as the poloidal circulation on the contour of the domain corresponding to $\mathcal{C}_q$. Deriving $\mathcal{C}_q$ and $\mathcal{H}_q$ with respect to q, we find that the distribution of the poloidal field $\mathcal{A}_q = \dfrac{1}{|\mathcal{D}|}\dfrac{\mathrm{d}\mathcal{C}_q}{\mathrm{d}q}$ together with the partial circulations $\mathcal{X}_q = \dfrac{1}{|\mathcal{D}|}\dfrac{\partial \mathcal{H}_q}{\partial q}$ are dynamical invariants of the axisymmetric equations.

The conservations of the areas $\mathcal{A}_q$ together with that of the partial circulations $\mathcal{X}_q$ is in fact equivalent to the conservations of the toroidal Casimirs together with the generalized helicities since for sufficiently regular functions f and g we can write C_f and H_g as

$$C_f\,[\sigma] = |\mathcal{D}| \int_{\mathbb{R}} \mathrm{d}q \mathcal{A}_q\,[\sigma]\, f(q) \text{ and } H_g\,[\sigma,\xi] = |\mathcal{D}| \int_{\mathbb{R}} \mathrm{d}q \mathcal{X}_q\,[\sigma,\xi]\, g(q). \tag{6}$$

Now, consider a discrete poloidal distribution, say $f(\sigma) = \sum_{k=1}^{K} \dfrac{A_k}{|\mathcal{D}|}\mathbf{1}_{\sigma=\sigma_k}$. Let $\mathfrak{S}_K = \{\sigma_1, \sigma_2 ... \sigma_K\}$ be the discretized set of possible values for the poloidal field. In this simplified yet general situation, the conservation of the Casimirs is equivalent to the conservation of the K areas and K partial circulations

$$\mathcal{A}_k\,[\sigma] = \int \mathbf{dx}\, \mathbf{1}_{\sigma(\mathbf{x})=\sigma_k} \text{ and } \mathcal{X}_k\,[\sigma,\xi] = \int \mathbf{dx}\, \xi \mathbf{1}_{\sigma(\mathbf{x})=\sigma_k}. \tag{7}$$

2.3 Discretization of the fluid and analogy with an Ising-like spin model

Discretization Let us cut a slice of fluid along a meridional plane $\mathcal{P}$, and draw a $N \times N$ regular lattice on it. We can consider a discretization of the toroidal field and the poloidal field $(\sigma_N, \xi_N) = (\sigma_{N,ij}, \xi_{N,ij})_{1\leq i,j\leq N}$. Each node of the grid corresponds to a position $(\mathbf{x_{N,ij}})$ in the physical space, on which there exist a two-degree-of-freedom object that we refer to as an elementary "Beltrami spin". One degree of freedom is related to the toroidal field, while the other is related to the poloidal field. The discretization procedure is sketched on Figure 1.

We associate to every spin configuration a discretized version of the axisymmetric energy (4), that is discretized into the sum of a toroidal energy and a poloidal energy, namely

$$\mathcal{E}[\sigma_N, \xi_N] = \mathcal{E}_{tor}[\sigma_N] + \mathcal{E}_{pol}[\xi_N] \tag{8}$$

$$\text{with } \mathcal{E}_{tor}[\sigma_N] = \frac{1}{4}\frac{|\mathcal{D}|}{N^2} \sum_{(i,j)\in[\![1;N]\!]^2} \frac{\sigma_{N,ij}^2}{y_i} \text{ and } \mathcal{E}_{pol}[\xi_N] = \frac{1}{2}\frac{|\mathcal{D}|}{N^2} \sum_{\substack{(i,j)\in[\![1;N]\!]^2 \\ (i',j')\in[\![1;N]\!]^2}} \xi_{N,ij} J_{iji'j'} \xi_{N,i'j'}. \tag{9}$$

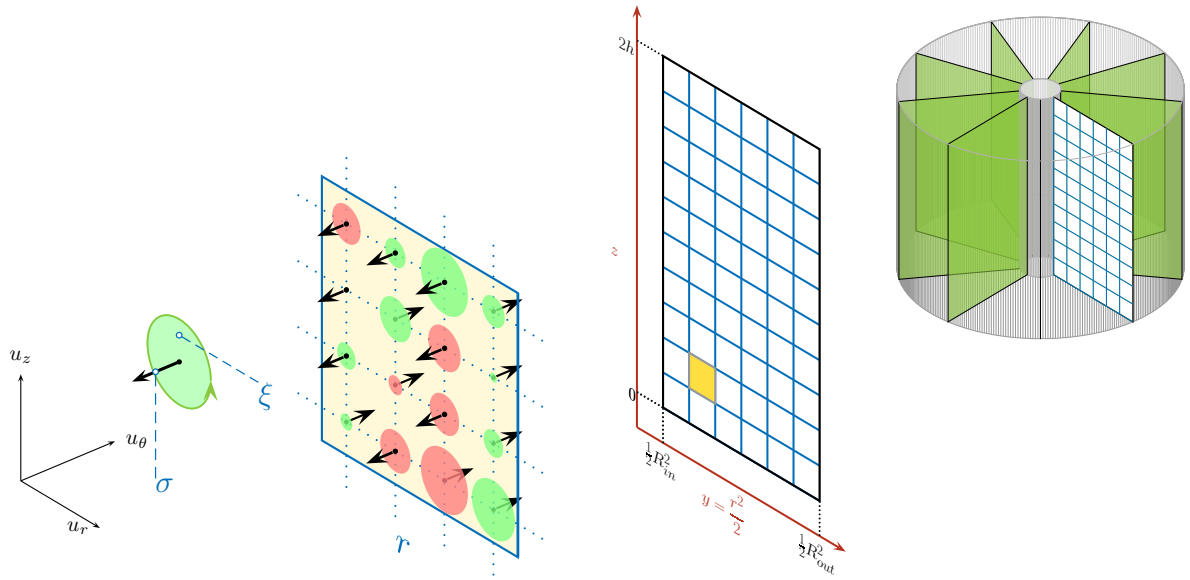

Figure 1: Discretization of the axisymmetric Euler equations onto an assembly of Beltrami spins (Impressionistic view). For each Beltrami spin, we represent the toroidal degree of freedom by an arrow, and the poloidal degree of freedom by a circle whose radius is proportionnal to the amplitude of the poloidal field. Red (green) circles denote negative (positive) vorticy.

$J_{iji'j'}$ denotes a discretized version of the operator $-(\Delta^\star)^{-1}$ with vanishing boundary conditions on the walls and periodic conditions along the vertical direction.

We also introduce the discretized version of the Casimir constraints (7) as

$$\mathcal{A}_k\left[\sigma_N\right] = \frac{|\mathcal{D}|}{N^2}\sum_{(i,j)\in[\![1;N]\!]^2}\mathbf{1}_{\sigma_{N,ij}=\sigma_k} \quad \text{and} \quad \mathcal{X}_k[\sigma_N,\xi_N] = \frac{|\mathcal{D}|}{N^2}\sum_{(i,j)\in[\![1;N]\!]^2}\xi_{N,ij}\mathbf{1}_{\sigma_{N,ij}=\sigma_k}. \tag{10}$$

Here, the indicator function $\mathbf{1}_{\sigma_{N,ij}=\sigma_k}$ is the function defined over the N^2 nodes of the grid, that takes value 1 when $\sigma_{N,ij}=\sigma_k$ and 0 otherwise.

For convenience we also introduce the discrete total poloidal circulation, $\mathcal{X}[\sigma_N,\xi_N] = \sum_{k=1}^{K}\mathcal{X}_k[\sigma_N,\xi_N]$.

To make the constraints more picturesque, we have sketched on Figure 2 different configurations of an assembly of four Beltrami spins with $K=2$, $\mathfrak{S}_2=\{-1,1\}$ corresponding to $A_1 = A_{-1} = \dfrac{|\mathcal{D}|}{2}$ and $X_1 = X_{-1} = 0$.

The microcanonical measure We consider the set $\mathcal{C}$ of $2K+1$ constraints given by

$$\mathcal{C} = \{E, \{A_k\}_{1\le k\le K}, \{X_k\}_{1\le k\le K}\}. \tag{11}$$

Given N, we define the configuration space $\mathcal{G}_N(E,\{A_k\},\{X_k\}) \subset (K\times\mathbb{R})^{N^2}$ the space of spin-configurations (σ_N,ξ_N) that are such that $E \le \mathcal{E}\left[\sigma_N,\xi_N\right] \le E+\Delta E$ and $\forall 1 \le k \le K$, $\mathcal{A}_k\left[\sigma_N\right] = A_k$, and $\mathcal{X}_k\left[\sigma_N,\xi_N\right] = X_k$. As will be clear later on, the number of

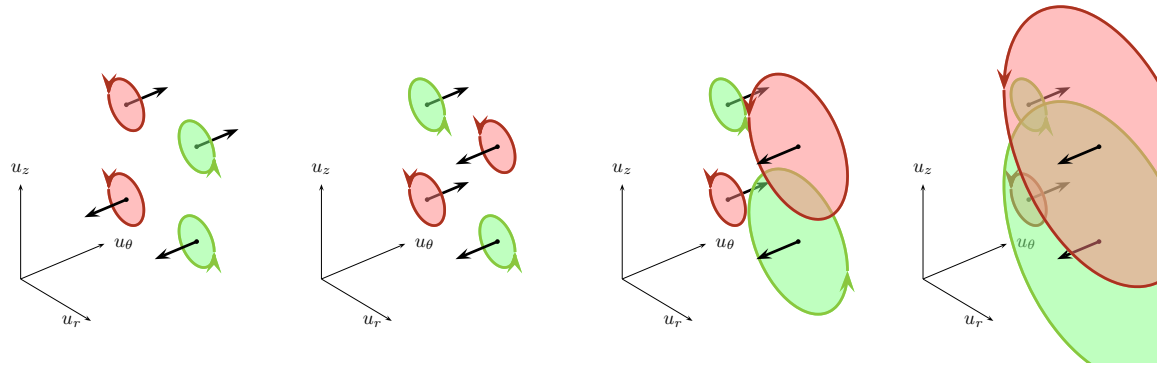

Figure 2: An assembly of four Beltrami Spins satisfying the same constraints on their toroidal Casimirs and partial circulations.

configurations will increase exponentially with N. Then in the limit of large N, due to this large deviation behavior, the microcanonical measure will not depend on ΔE.

Because the poloidal degrees of freedom may make $\mathcal{G}_N$ infinite, we also introduce the bounded ensembles $\mathcal{G}_{M,N}$ made of the spin-configurations of $\mathcal{G}_N$ that satisfy $(\sup_{ij} |\xi_{N,ij}| \leq M)$. For every ensemble $\mathcal{G}_{M,N}$, we can then define a M, N dependent microcanonical measure $\mathrm{d}\mathcal{P}_{M,N}$ together with a M, N dependent microcanonical average $<>_{M,N}$ by assigning a uniform weight to the spin configurations in $\mathcal{G}_{M,N}$. The construction of $\mathrm{d}\mathcal{P}_{M,N}$ and $<>_{M,N}$ is explicitly carried out in sections (3.1) and (4.1).

The present paper aims at building a thermodynamic limit by letting successively $(N \to \infty)$ and $(M \to \infty)$ for this set of microcanonical measures, and to describe this limit. We will refer to this problem as problem $\mathcal{P}$. Let us emphasize, that the two limits $(N \to \infty)$ and $(M \to \infty)$ most probably do not commute. We argue that the relevant limit is the limit $(N \to \infty)$ first. Taking the limit $(N \to \infty)$ first, we make sure that we describe a microcanonical measure that corresponds to the dynamics of a continuous field (a fluid). The microcanonical measure at fixed M then corresponds to an approximate invariant measure, for which the maximum value of the vorticity is limited. Such a fixed M measure could be relevant as a large, but finite time approximation if the typical time to produce large values of the vorticity is much longer than the typical time for the turbulent mixing. Finally, for infinite time, we recover the microcanonical measure by taking the limit $(M \to \infty)$. For these reasons, we think that the physical limit is the limit $(N \to \infty)$ first.

As for the physics we want to understand, it is the following. Consider an assembly of Beltrami spins with a given energy E. What is the fraction of E that typically leaks into the toroidal part and into the poloidal part ? What does a typical distribution of Beltrami spins then look like ?

2.4 How is the microcanonical measure related to the axisymmetric Euler equations ?

Interpreting the invariants as geometrical constraints on a well- defined assembly of spin-like objects allowed us to map the microcanonical measure of discretized hydrodynamical fields and invariants to an "Ising-like model". Taking the thermodynamical limit $(N \to \infty)$ allows to retrieve continuous hydrodynamical fields and invariants. How is the limit microcanonical measure related to the axisymmetric Euler equations ? Is it an invariant measure of the axisymmetric Euler equations ?

The answer is positive but not trivial. The very reason why this should be true relies in the existence of a formal Liouville theorem – *i.e.* an extension of Liouville theorem for infinite dimensional Hamiltonian systems – for the axisymmetric Euler equations. An elementary proof concerning the existence of a formal Liouville theorem can be found in [Thalabard, 2013]. This formal Liouville theorem guarantees that the thermodynamic limit taken in a microcanonical ensemble induces an invariant measure of the full axisymmetric equations.

The same issue arises in the simpler framework of the 2D Euler equations. A similar mapping onto a system of vortices that behaves as a mean-field Potts model, and definition of the microcanonical measure is can be found in [Miller, 1990, Ellis et al., 2004, Bouchet and Venaille, 2011]. In [Bouchet and Corvellec, 2010], it is discussed why the microcanonical measure is an invariant measure of the 2D Euler equations. The proof is adaptable to the axisymmetric case but goes beyond the scope of the present paper.

It is thus expected that the microcanonical measure of ensembles of Beltrami spins is an invariant measure of the Euler axisymmetric equations, therefore worth of interest. This motivates the present study.

3 Statistical mechanics of a simplified problem without helical correlations

Before tackling the full problem, we investigate a simplified instance of the problem, where the toroidal part is entirely decoupled from the poloidal part. This is a much simpler case whose results will prove fruitful to understand the full problem.

3.1 Definition of the simplified problem

It is illuminating to look beforehands at a slightly modified version of problem $\mathcal{P}$ obtained by replacing the K constraints on the partial circulations by a single contraint on the total circulation X_{tot}. This new problem will be much simpler to understand and can be completely worked out analytically. The set of $2K+1$ constraints $\mathcal{C}$ is here replaced by a set $\tilde{\mathcal{C}}$ of $K+2$ constraints, defined as

$$\tilde{\mathcal{C}} = \{E, \{A_k\}_{1\leq k\leq K}, X_{tot} = \sum_{k=1}^{K} X_k\}. \tag{12}$$

In this new problem $\tilde{\mathcal{P}}$, the correlations between the toroidal field and the poloidal field due to the toroidal Casimirs and the generalized helicities disappear. The only coupling left between those two fields is a purely thermal one: the only way the fields can mutually interact is by exchanging some energy between each other. In order to make this statement more rigorous, we now need to get into some finer details and build the microcanonical measure for problem $\tilde{\mathcal{P}}$. This is the subject of the next paragraph.

3.1.1 Explicit construction of the microcanonical measure

In order to exhibit a configuration of Beltrami spins (σ_N, ξ_N) that satisfies the constraints $\tilde{\mathcal{C}}$, it suffices to pick a toroidal configuration $\sigma_N = (\sigma_{N,ij})_{1\leq i,j\leq N}$ with areas A_k and toroidal energy E_{tor} together with a poloidal configuration $\xi_N = (\xi_{N,ij})_{1\leq i,j\leq N}$ with a poloidal

circulation X_{tot} and poloidal energy $E_{pol} = E - E_{tor}$. It is thus natural to introduce the toroidal spaces of configurations $\mathcal{G}_N^{tor}(E, \{A_k\})$ together with the poloidal spaces of configurations $\mathcal{G}_{M,N}^{pol}(E, X_{tot})$ defined as

$$\mathcal{G}_N^{tor}(E, \{A_k\}) = \{\sigma_N \in \mathfrak{S}_K^{N^2} \mid \mathcal{E}_{tor}(\sigma_N) = E \text{ and } \forall k \in [\![1; K]\!]\, \mathcal{A}_k[\sigma_N] = A_k\}, \quad (13)$$

$$\text{and } \mathcal{G}_{M,N}^{pol}(E, X_{tot}) = \{\xi_N \in [-M; M]^{N^2} \mid \mathcal{E}_{pol}(\xi_N) = E \text{ and } \mathcal{X}[\xi_N] = X_{tot}\}. \quad (14)$$

For finite N, there is only a finite number of toroidal energies E_{tor} for which the space of toroidal configurations $\mathcal{G}_N^{tor}(E, \{A_k\})$ is non empty. The space of bounded Beltrami-spin configurations $\mathcal{G}_{M,N}(E, \{A_k\})$ is then simply a finite union of disjoint ensembles, that can be formally written as

$$\mathcal{G}_{M,N}(E, \{A_k\}, X_{tot}) = \bigcup_{0 \le E_{tor} \le E} \mathcal{G}_N^{tor}(E_{tor}, \{A_k\}) \times \mathcal{G}_{M,N}^{pol}(E - E_{tor}, X_{tot}). \quad (15)$$

Definition of the M, N-dependent microcanonical measure The M, N- dependent microcanonical measure $\mathrm{d}\mathcal{P}_{M,N}$ is defined as the uniform measure on the space of configurations $\mathcal{G}_{M,N}(E, \{A_k\}, X_{tot})$. In order to specify this measure explicitly, we need to define the M, N-dependent volume $\Omega_{M,N}(E, \{A_k\}, X_{tot})$ of $\mathcal{G}_{M,N}(E, \{A_k\}, X_{tot})$. To do so, we write $\Omega_N^{tor}(E, \{A_k\})$ the number of configurations in $\mathcal{G}_N^{tor}(E, \{A_k\})$ and $\Omega_N^{pol}(E, X_{tot})$ the hypervolume in $\mathbb{R}^{N^2}$ of $\mathcal{G}_{M,N}^{pol}(E, X_{tot})$, so that

$$\Omega_N^{tor}(E, \{A_k\}) = \sum_{\sigma_N \in \mathfrak{S}_K^{N^2}} \mathbf{1}_{\sigma_N \in \mathcal{G}_N^{tor}(E, \{A_k\})}, \quad (16)$$

$$\text{and } \Omega_{M,N}^{pol}(E, X_{tot}) = \prod_{(i,j) \in [\![1;N]\!]^2} \int_{-\infty}^{+\infty} \mathrm{d}\xi_{N,ij} \mathbf{1}_{\xi_N \in \mathcal{G}_{M,N}^{pol}(E, X_{tot})}. \quad (17)$$

Note that the integral defining the poloidal volume is finite since $\mathcal{G}_{M,N}^{pol}(E, X_{tot})$ is a bounded subset of $\mathbb{R}^{N^2}$. Using equation (15), the phase-space volume can then be written as

$$\Omega_{M,N}(E, \{A_k\}, X_{tot}) = \int_0^E \mathrm{d}E_{tor}\, \Omega_N^{tor}(E_{tor}, \{A_k\})\, \Omega_{M,N}^{pol}(E - E_{tor}, X_{pol}). \quad (18)$$

The microcanonical weight $\mathrm{d}\mathcal{P}_{M,N}(\mathcal{C})$ of a configuration $\mathcal{C} = (\sigma_N, \xi_N)$ lying in the space $\mathcal{G}_{M,N}(E, \{A_k\}, X_{tot})$ can now be explicitly written as

$$\mathrm{d}\mathcal{P}_{M,N}(\mathcal{C}) = \frac{1}{\Omega_{M,N}(E, \{A_k\}, X_{tot})} \prod_{(i,j) \in [\![1;N]\!]^2} \mathrm{d}\xi_{N,ij}. \quad (19)$$

Provided that $\mathcal{G}$ is a compact subset of ${\mathfrak{S}_K}^{N^2} \times \mathbb{R}^{N^2}$ it is convenient to use the shorthand notation

$$\int_{\mathcal{G}} \mathrm{d}\mathcal{P}_{M,N} \equiv \frac{1}{\Omega_{M,N}(E, \{A_k\}, X_{tot})} \sum_{\sigma_N \in \mathfrak{S}_K^{N^2}} \left(\prod_{(i,j) \in [\![1;N]\!]^2} \int_{-\infty}^{\infty} \mathrm{d}\xi_{N,ij} \right) \mathbf{1}_{(\sigma_N, \xi_N) \in \mathcal{G}}, \quad (20)$$

so that the M, N dependent microcanonical average $<>_{M,N}$ of an observable $\mathcal{O}$ can now be defined as

$$\langle \mathcal{O} \rangle_{M,N} = \int_{\mathcal{G}_{M,N}(E, \{A_k\}, X_{tot})} \mathrm{d}\mathcal{P}_{M,N}\, \mathcal{O}[\sigma_N, \xi_N] = \int_0^E \mathrm{d}E_{tor} \int_{\mathcal{G}_N^{tor}(E_{tor}, \{A_k\}) \times \mathcal{G}_{M,N}^{pol}(E - E_{tor}, X_{tot})} \mathrm{d}\mathcal{P}_{M,N}\, \mathcal{O}[\sigma_N, \xi_N]. \quad (21)$$

Definition of the limit measures It is convenient to use observables to define the limit microcanonical measures. We define the M-dependent microcanonical measure $<>_M$ and the microcanonical measure $<>$ by letting successively $N \to \infty$ and $M \to \infty$, so that for any observable $\mathcal{O}$, $< \mathcal{O} >_M$ and $< \mathcal{O} >$ are defined as

$$\langle \mathcal{O} \rangle_M = \lim_{N \to \infty} \langle \mathcal{O} \rangle_{M,N}, \text{ and } \langle \mathcal{O} \rangle = \lim_{M \to \infty} \langle \mathcal{O} \rangle_M. \tag{22}$$

3.1.2 Observables of physical interest

Without any further comment about observables and the kind of observables that we will specifically consider, equations (21) and (22) may appear to be slightly too casual. Let us precise what we mean. In our context, we need to deal both with observables defined for the continuous poloidal and toroidal fields and for their discretized counterparts. Given a continuous field (σ, ξ) we consider observables $\mathcal{O}$ that can be written as $\mathcal{O} = \int_{\mathcal{D}} \mathbf{dx}\, f^{\mathcal{O}}_{(\mathbf{x})}(\sigma, \xi)$ where $f^{\mathcal{O}}_{(\mathbf{x})}$ is a function defined over ${\mathfrak{S}_K}^{\mathcal{D}} \times \mathbb{R}^{\mathcal{D}} \times \mathcal{D}$. The discrete counterpart of $\mathcal{O}$ is then defined as

$$\mathcal{O}(\sigma_N, \xi_N) = \frac{|\mathcal{D}|}{N^2} \sum_{(i,j) \in [\![1;N]\!]^2} f^{\mathcal{O}}_{\left(\mathbf{x_{N,ij}}\right)}(\sigma_N, \xi_N), \tag{23}$$

and the distinction between discrete and continuous observables is made clear from the context.

To learn about the physics described by the microcanonical measure, a first non trivial functionnal to consider is the toroidal energy functionnal $\mathcal{E}_{tor}$ defined in equation (9), whose microcanonical average will tell what the balance between the toroidal and poloidal energy for a typical configuration Beltrami spins is. In order to specify the toroidal and poloidal distributions in the thermodynamic limit we will then estimate the microcanonical averages of specific one-point observables, namely

$$\mathcal{O}(\{\sigma\}, \{\xi\}) = \int_{\mathcal{D}} \mathbf{dx}\, \delta(\mathbf{x} - \mathbf{x_0})\, \sigma(\mathbf{x})^p\, \xi(\mathbf{x})^k = \mathcal{O}^{tor}(\{\sigma\}) \mathcal{O}^{pol}(\{\xi\}) \tag{24}$$

with $\mathcal{O}^{tor}(\{\sigma\}) = \sigma(\mathbf{x_0})^p$ and $\mathcal{O}^{pol}(\{\xi\}) = \xi(\mathbf{x_0})^k$ defined for any point $(\mathbf{x_0}) \in \mathcal{D}$. The microcanonical averages of those observables provide the moments of the one-point probability distributions and therefore fully specify them. [1]

Just as for the 2D Euler equations, and slightly anticipating on the actual computation of the microcanonical measures, we can expect the axisymmetric microcanonical measures to behave as Young measures, that is to say that the toroidal and poloidal distributions at positions $(\mathbf{x})$ are expected to be independent from their distributions at position $(\mathbf{x}') \neq (\mathbf{x})$. Therefore, specifying the one-point probability distributions will hopefully suffice to completely describe the statistics of the poloidal and of the toroidal field in the thermodynamic limit.

3.1.3 Specificity of problem $\tilde{\mathcal{P}}$

Looking at equation (21), it is yet not so clear that problem $\tilde{P}$ is easier to tackle than problem $\mathcal{P}$, nor that the limit measures prescribed by equation (22) can be computed.

[1] One can observe that one-point moments may be ill-defined in the discrete case so that their limit may be ill-defined too. One way to deal with this situation is to consider dyadic discretizations, namely choose $N = 2^n$. Then for any point $(\mathbf{x})$ whose coordinates are dyadic rationnal numbers, the discretized quantities are non trivially zero when n is large enough. The microcanonical averages can then be extended to any position in $\mathcal{D}$ by continuity.

The reason why we should keep hope owes to large deviation theory. Using classical arguments from statistical physics we argue hereafter that problem $\mathcal{P}$ can be tackled by defining appropriate poloidal and toroidal measures that can be studied separately from each other.

Let us for instance consider the Boltzmann entropies per spin

$$S_N^{tor}(E,\{A_k\}) = \frac{1}{N^2}\log\Omega_N^{tor}(E,\{A_k\}), \quad S_{M,N}^{pol}(E,X_{tot}) = \frac{1}{N^2}\log\Omega_N^{pol}(E,X_{tot}), \tag{25}$$

$$\text{and} \quad S_{M,N}(E,\{A_k\},X_{tot}) = \frac{1}{N^2}\log\Omega_N(E,\{A_k\},X_{tot}). \tag{26}$$

As $N\to\infty$, it can be expected that the toroidal entropies $S_N^{tor}(E,\{A_k\})$ together with the poloidal entropies $S_{M,N}^{pol}(E,X_{tot})$ converge towards a finite limit if they are properly renormalized. If this is the case, then those entropies can be asymptotically expanded as

$$S_N^{tor}(E,\{A_k\}) \underset{N\to\infty}{=} c_N^{tor}(\{A_k\}) + S^{tor}(E,\{A_k\}) + o(1), \tag{27}$$

$$\text{and} \quad S_{M,N}^{pol}(E,X_{tot}) \underset{N\to\infty}{=} c_{M,N}^{pol}(X_{tot}) + S_M^{pol}(E,X_{tot}) + o(1). \tag{28}$$

Plugging the entropies into equation (18), we get, when $N\to\infty$

$$\Omega_{M,N}(E) = e^{N^2\left(c_N^{tor}+c_{M,N}^{pol}\right)+o(N^2)}\int_0^E \mathrm{d}E_{tor}\,\mathrm{e}^{N^2\left(S^{tor}(E_{tor})+S_M^{pol}(E-E_{tor})\right)}. \tag{29}$$

For clarity, we have not mentionned the $\{A_k\}$ and X_{tot} dependence of the different entropies. Using Laplace's method to approximate integrals, taking logarithm of both sides of equation (29), dividing by N^2, and setting $c_{M,N}(\{A_k\},X_{tot}) = c_N^{tor}(\{A_k\}) + c_{M,N}^{pol}(X_{tot})$ we obtain

$$S_{M,N}(E) \underset{N\to\infty}{=} c_{M,N} + S^{tor}(E_M^\star) + S_M^{pol}(E-E_M^\star) + o(1),$$

$$\text{where } E_M^\star = \underset{x\in[0;E]}{\arg\max}\{S^{tor}(x) + S_M^{pol}(E-x)\}. \tag{30}$$

A heuristic way of interpreting equation (30) is to say that when $N\gg 1$, "most of" the configurations in $\mathcal{G}_{M,N}(E,\{A_k\},X_{tot})$ have a toroidal energy equal to $E_M^\star$ and a poloidal energy equal to $E-E_M^\star$.

We can refine the argument, and ask what the typical value of a one-point observable $\mathcal{O} = \mathcal{O}^{tor}\mathcal{O}^{pol}$ as described in equation (24) becomes in the thermodynamic limit $N\to\infty$.

Let us then introduce the M,N dependent toroidal and poloidal partial microcanonical measures as

$$\mathrm{d}\mathcal{P}_N^{tor,E}(\sigma_N) = \frac{1}{\Omega_N^{tor}(E,\{A_k\})} \text{ and } \mathrm{d}\mathcal{P}_{M,N}^{pol,E}(\xi_N) = \frac{1}{\Omega_{M,N}^{pol}(E,X_{tot})}\prod_{(i,j)\in[\![1;N]\!]^2}\mathrm{d}\xi_{N,ij}, \tag{31}$$

together with the shorthand notations

$$\int_{\mathcal{G}}\mathrm{d}\mathcal{P}_N^{tor,E} \equiv \frac{1}{\Omega_N^{tor}(E,\{A_k\})}\sum_{\sigma_N\in\mathfrak{S}_K^{N^2}}\mathbf{1}_{\sigma_N\in\mathcal{G}},$$

$$\text{and} \int_{\mathcal{G}}\mathrm{d}\mathcal{P}_{M,N}^{pol,E} \equiv \frac{1}{\Omega_{M,N}^{pol}(E,X_{tot})}\left(\prod_{(i,j)\in[\![1;N]\!]^2}\int_{-\infty}^{\infty}\mathrm{d}\xi_{N,ij}\right)\mathbf{1}_{\xi_N\in\mathcal{G}}. \tag{32}$$

Respectively defining the M, N dependent toroidal and poloidal partial microcanonical means as

$$\langle \mathcal{O}^{tor} \rangle_N^{tor,E} = \int_{\mathcal{G}_N^{tor}(E,\{A_k\})} \mathrm{d}\mathcal{P}_N^{tor,E}\, \mathcal{O}^{tor}\left[\sigma_N\right] \quad \text{and} \quad \langle \mathcal{O}^{pol} \rangle_{M,N}^{pol,E} = \int_{\mathcal{G}_{M,N}^{pol}(E,X_{tot})} \mathrm{d}\mathcal{P}_{M,N}^{pol,E}\, \mathcal{O}^{pol}\left[\xi_N\right], \tag{33}$$

it stems from equation (21) that

$$\langle \mathcal{O} \rangle_{M,N} = \int_0^E \mathrm{d}E_{tor}\, \mathcal{P}_{M,N}(E_{tor})\, \langle \mathcal{O}^{tor} \rangle_N^{tor,E_{tor}}\, \langle \mathcal{O}^{pol} \rangle_{M,N}^{pol,E-E_{tor}}, \tag{34}$$

$$\text{with} \quad \mathcal{P}_{M,N}(E_{tor}) = \frac{\Omega_N^{tor}(E_{tor})\, \Omega_{M,N}^{pol}(E - E_{tor})}{\Omega_{M,N}(E)}. \tag{35}$$

The latter equation means that the full microcanonical measure $<>_{M,N}$ can be deduced from the knowledge of the partial measures $<>_N^{tor,E}$ and $<>_{M,N}^{pol,E}$. As $N \to \infty$, the limit measure can be expected to be dominated by one of the partial measures, provided that the limit measures $<>^{tor,E}$, $<>_M^{pol,E}$ – defined accordingly to equation (22) behave as predicted by equations (27) and (28).

If for example one considers an observable $\mathcal{O}$ that is bounded independently from N , then its limit microcanonical mean can be estimated from equation (34) as

$$\langle \mathcal{O} \rangle_M = \langle \mathcal{O}^{tor} \rangle^{tor,E_M^\star}\, \langle \mathcal{O}^{pol} \rangle_M^{pol,E-E_M^\star}. \tag{36}$$

Thermodynamically stated, this means that the statistical equilibria related to problem $\tilde{\mathcal{P}}$ can be interpreted as thermal equilibria between the toroidal field and the poloidal field. It is therefore relevant to study separately the typical toroidal configurations and the typical poloidal configurations in order to understand what the typical configurations of Beltrami spins configurations are depending of the constraints $\tilde{\mathcal{C}}$. This is what we do in the next three sections.

3.2 Statistical mechanics of the toroidal field

It is possible to estimate the toroidal entropies $S_N^{tor}(E, \{A_k\})$ for very specific values of the energy using common counting in statistical mechanics. We first present those. Then, we show that those specific cases are retrieved with a more general calculation involving a large deviation theorem.

3.2.1 Traditionnal counting

The contribution to the toroidal energy of a toroidal spin $\sigma_{k_0} \in \mathfrak{S}_K$ placed at a radial distance $y = \dfrac{r^2}{2}$ from the center of the cylinder is $\dfrac{|\mathcal{D}|\, \sigma_{k_0}^2}{4yN^2}$. Clearly, the energy is extremal when the σ_k^2 are fully segregated in K stripes, parallel to the z axis, each of width $w_k = \dfrac{(R_{out}^2 - R_{in}^2)\, A_k}{2\,|\mathcal{D}|} + O\left(\dfrac{1}{N}\right)$. The minimum (resp. maximum) of energy $E_{\min}$ (resp. $E_{\max}$) is obtained when the levels of σ_k^2 are sorted increasingly (resp. decreasingly) from the internal cylinder. The number of toroidal configurations that corresponds to each one of those extremal energy states is therefore at most of order N. Using definition (25) and equation (27) , one therefore finds $S^{tor}(E_{\min}, \{A_k\}) = S^{tor}(E_{\max}, \{A_k\}) = 0$.

Further assuming that $S^{tor}(E,\{A_k\})$ is sufficiently regular on the interval $[E_{\min};E_{\max}]$, the latter result implies that there exists an energy value $E^\star \in [E_{\min};E_{\max}]$ for which the entropy $S^{tor}(E,\{A_k\})$ is maximal. The value of $S^{tor}(E^\star,\{A_k\})$ can be estimated by counting the total number of toroidal configurations – regardless of their toroidal energies [2]. Indeed,

$$\frac{N^2!}{\prod_{k=1}^K N_k!} = \int_{E_{\min}}^{E_{\max}} \mathrm{d}E\, \Omega_N^{tor}(E,\{A_k\}) = \int_{E_{min}}^{E_{max}} \mathrm{d}E\, e^{N^2 S_N^{tor}(E,\{A_k\})}, \tag{37}$$
$$\text{where } N_k = \frac{N^2 A_k}{|\mathcal{D}|}.$$

Then, taking the limit $N \to \infty$, using Stirling formula for the l.h.s and estimating the r.h.s with the method of steepest descent, we obtain

$$S^{tor}(E^\star,\{A_k\}) = -\sum_{k=1}^K \frac{A_k}{|\mathcal{D}|} \log \frac{A_k}{|\mathcal{D}|}. \tag{38}$$

This value corresponds to the levels of σ_k^2 being completely intertwined.

3.2.2 Large deviation approach

We can work out the entropy for any value of the energy by using the more modern framework of large deviation theory.

For a given N, let us consider the set of random toroidal configurations that can be obtained by randomly and independently assigning on each node of the lattice a level of σ_k drawn from a uniform distribution over the discrete set $\mathfrak{S}_K$. There are K^{N^2} such different configurations. Among those, there exist some that are such that $\forall k \in [\![1;K]\!]\, \mathcal{A}_k[\sigma_N] = A_k$ together with $\mathcal{E}^{tor}[\sigma_N] = E$. The number of those configurations is precisely what we have defined as $\Omega_N^{tor}(E,\{A_k\})$. Can we estimate $\Omega_N^{tor}(E,\{A_k\})$ for $N \gg 1$? The answer is provided by a large deviation theorem called Sanov theorem (see Appendix E for a detailed statement of the theorem).

Through a coarse graining, we define the local probability $p_k(\mathbf{x})$ that a toroidal spin takes the value σ_k in an infinitesimal area $\mathbf{dx}$ around a point $(\mathbf{x})$. With respect to the ensemble of configurations, the functions $(p_1,...,p_K)$ define a toroidal macrostate. Each macrostate therefore satisfies the local normalization constraint:

$$\forall \mathbf{x} \ \in \mathcal{D}, \sum_{k=1}^K p_k(\mathbf{x}) = 1. \tag{39}$$

We denote $\mathcal{Q}^{tor}$ the set of all the toroidal macrostates – the set of all $p = (p_1,...,p_K)$ verifying (39). As explained in Appendix E, from Sanov theorem we can compute the number of configurations corresponding to the macrostate $p = (p_1,...,p_K)$. This number is equivalent for large N to N^2 times the exponential of the macrostate entropy

$$\mathcal{S}^{tor}[p] = -\frac{1}{|\mathcal{D}|}\int_{\mathcal{D}} \mathbf{dx} \sum_{k=1}^K p_k(\mathbf{x}) \log p_k(\mathbf{x}). \tag{40}$$

[2]We here tacitly work in the case where the σ_k^2 are all distinct –otherwise we need to group the levels with the same value of σ_k^2.

The constraints on the area A_k occupied by each level σ_k of the toroidal variable, and the toroidal energy constraint, can be expressed as linear constraints on the toroidal macrostates:

$$\forall k \in [\![1;K]\!]\, \mathcal{A}_k[p] = \int_{\mathcal{D}} \mathbf{dx}\, p_k(\mathbf{x}) \text{ and } \mathcal{E}_{tor}[p] = \int \mathbf{dx} \sum_{k=1}^{K} p_k(\mathbf{x}) \frac{\sigma_k^2}{4y}, \tag{41}$$

where $\mathcal{E}_{tor}[p]$ and $\mathcal{A}_k[p]$ are the energy and areas of a macrostate $p = (p_1, ..., p_K)$. As the log of the entropy is proportional to the number of configurations, the most probable toroidal macrostate will maximize the macrostate entropy (40) with the constraints $\forall k \in [\![1;K]\!]$, $\mathcal{A}_k[p] = A_k$ and $\mathcal{E}_{tor}[p] = E$. Moreover, using Laplace method of steepest descent, we can conclude that in the limit of large N, the total entropy is equal to the entropy of the most probable macrostate. Therefore,

$$S^{tor}(E, \{A_k\}) = \lim_{N\to\infty} \frac{1}{N^2} \log \Omega_N^{tor}(E, \{A_k\}) \tag{42}$$

$$= \sup_{p\in\mathcal{Q}^{tor}} \{\mathcal{S}^{tor}[p] \mid \forall k \in [\![1;K]\!]\, \mathcal{A}_k[p] = A_k \text{ and } \mathcal{E}_{tor}[p] = E\}. \tag{43}$$

The optimization problem which appears in the r.h.s. of equation (43) can be solved using some Lagrange multipliers α_k and β_{tor} to respectively enforce the constraints on the areas A_k and the energy E. The critical points $p^{\star,E}$ of the macrostate entropy for the constraints E and A_k can then be written as

$$p_k^{\star,E}(\mathbf{x}) = \frac{1}{Z^\star(\mathbf{x})} \exp\{\alpha_k - \beta\frac{\sigma_k^2}{4y}\} \text{ with } Z^\star(\mathbf{x}) = \sum_{k=1}^{K} \exp\{\alpha_k - \beta\frac{\sigma_k^2}{4y}\}. \tag{44}$$

α_k and β_{tor} are such that

$$\int_{\mathcal{D}} \mathbf{dx} \frac{\partial \log Z^\star(\mathbf{x})}{\partial \alpha_k} = A_k \text{ and } -\int_{\mathcal{D}} \mathbf{dx} \frac{\partial \log Z^\star(\mathbf{x})}{\partial \beta_{tor}} = E. \tag{45}$$

Note that if we don't enforce the energy constraint in (43), it is easily checked that the maximum value of the macrostate entropy is $\mathcal{S}^{tor}[p^\star] = -\sum_{k=1}^{K} \frac{A_k}{|\mathcal{D}|} \log \frac{A_k}{|\mathcal{D}|}$ obtained for the macrostate p defined by $p_k^\star(\mathbf{x}) = \frac{A_k}{|\mathcal{D}|}$. This shows the consistency of our calculation since the latter macrostate can also be found by setting $\beta_{tor} = 0$ in (45). A vanishing β_{tor} corresponds to the energy constraint $E = E^\star$, so that $S^{tor}(E^\star, \{A_k\}) = -\sum_{k=1}^{K} \frac{A_k}{|\mathcal{D}|} \log \frac{A_k}{|\mathcal{D}|}$, and equation (38) is retrieved. The value of $E^\star$ can be computed from (41) and (45) as $E^\star = \sum_{k=1}^{K} \frac{A_k \sigma_k^2}{2|\mathcal{D}|} \log \frac{R_{out}}{R_{in}}$.

Equation (45) can also be used to numerically estimate the toroidal entropy for abitrary values of E. Such an estimation is shown on Figure 3 for the specific case where $K = 2$, $\mathfrak{S}_2 = \{0, 1\}$, and $A_0 = A_1 = \frac{|\mathcal{D}|}{2}$.

Finally, the microcanonical toroidal moments can be deduced from the critical distribution $p^{\star,E}$ that achieves the maximum macrostate entropy. Those moments read

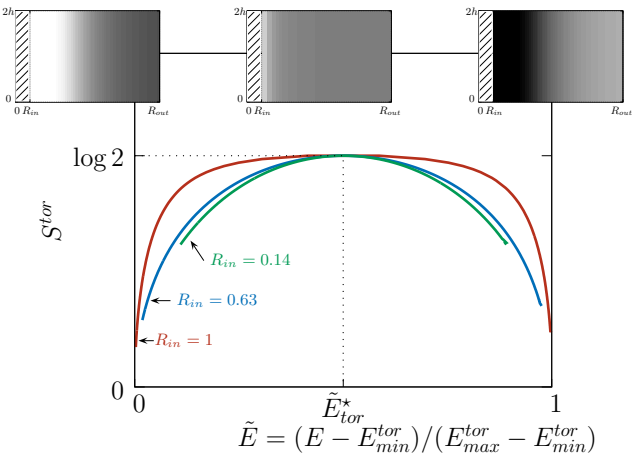

Figure 3: Numerical estimation of the toroidal entropy for K=2 , $\mathfrak{S}_2 = \{0, 1\}$ and $A_0 = A_1 = \frac{\mathcal{D}}{2}$. The height of the domain is $2h = 1$, its outer radius is $R_{out} = \sqrt{2}$ and its inner radius is $R_{in} = 0.14$,0.63 or 1. Insets show typical toroidal fields $\langle \sigma(\mathbf{x}) \rangle^{tor,E}$ for $R_{in} = 0.14$. They correspond to $E = 0.1$, $E = 0.5$, and $E = 0.9$ from left to right. The grayscale ranks from 0 (white pixels) to 1 (black pixels).

$$\langle \sigma(\mathbf{x})^p \rangle^{tor,E} = \sum_{k=1}^{K} p_k^{\star,E}(\mathbf{x}) \, \sigma_k^p. \tag{46}$$

In the thermodynamic limit, the microcanical measure $<>^{tor,E} = \lim_{N\to\infty} <>_N^{tor,E}$ behaves as a product measure, so that equation (46) completely describes the toroidal micocanonical measure.

3.3 Statistical mechanics of the poloidal field

3.3.1 Computation of the M-dependent partial measures $<>_M^{pol,E}$

Dealing with the partial poloidal measure is slightly more subtle. The problem is that the poloidal energy constraint cannot be exactly expressed as a constraint on the poloidal macrostates. We however argue that Sanov therorem can still be applied because the poloidal degrees of freedom interact through long range interactions, which gives the poloidal problem a mean-field behavior.

We consider the set of random poloidal configurations that can be obtained by randomly and independently assigning on each node of the lattice a random value of ξ from the uniform distribution over the interval $[-M, M]$. We then define through a coarse graining the local probability $p_M(\xi, \mathbf{x})$ that a poloidal spin takes a value between ξ and $\xi + \mathrm{d}\xi$ in an infinitesimal area $\mathbf{dx}$ around a point $(\mathbf{x})$. With respect to the ensemble of poloidal configurations, the distributions $p_M = \{p_M(\xi, \cdot)\}_{\xi \in [-M;M]}$ define a poloidal macrostate. Each poloidal macrostate satisfies the local normalization constraint :

$$\forall \mathbf{x} \ \in \mathcal{D}, \int_{-M}^{M} \mathrm{d}\xi p_M(\xi, \mathbf{x}) = 1. \tag{47}$$

We denote $\mathcal{Q}^{pol}$ the sets of all the poloidal macrostates – the set of all p_M verifying (47). The number of configurations corresponding to the macrostate p_M is then N^2 times the exponential of the poloidal macrostate entropy

$$\mathcal{S}_M^{pol}[p_M] = -\frac{1}{|\mathcal{D}|}\int_{\mathcal{D}} \mathbf{dx} \int_{-M}^{M} \mathrm{d}\xi p_M(\xi, \mathbf{x}) \log p_M(\xi, \mathbf{x}). \tag{48}$$

The constraint on the total circulation X_{tot} can be expressed as a linear constraint on the poloidal macrostates

$$\mathcal{X}_{tot}[p_M] = \int_{\mathcal{D}} \mathbf{dx} \int_{-M}^{M} \mathrm{d}\xi\, \xi p_M(\xi, \mathbf{x}). \tag{49}$$

The subtle point arises when dealing with the constraint on the poloidal energy. The energy of a poloidal macrostate is defined as

$$\mathcal{E}^{pol}[p_M] = \frac{1}{2}\int_{\mathcal{D}} \mathbf{dx}\, \psi(\mathbf{x}) \int_{-M}^{M} \mathrm{d}\xi\, \xi p_M(\xi, \mathbf{x}), \tag{50}$$

$$\text{with} \quad \psi(\mathbf{x}) = \int_{\mathcal{D}} \mathbf{dx}' G(\mathbf{x}, \mathbf{x}') \langle \xi(\mathbf{x}') \rangle_{\mathbf{M}}^{\mathbf{pol}}, \tag{51}$$

$G(\mathbf{x}, \mathbf{x}')$ being the Green function of the operator $-\Delta^\star$ with vanishing boundary conditions on the walls and periodic boundary conditions along the vertical direction. The energy $\mathcal{E}[\xi_N]$ of a poloidal configuration (9) is therefore not exactly the energy of the corresponding macrostate (50). In order to deal with this situation, one needs to make the coarse-graining procedure more explicit. Dividing the $N \times N$ lattices into $N_b \times N_b$ contiguous blocks each composed of $n^2 = \lfloor N/N_b \rfloor^2$ spins, and taking the limit $N \to \infty$ at fixed N_b, and then letting $N_b \to \infty$, one obtains

$$\mathcal{E}^{pol}[\xi_N] \underset{\substack{N\to\infty \\ N_b\to\infty}}{=} \mathcal{E}^{pol}[p_M] + o\left(\frac{1}{N_b^2}\right). \tag{52}$$

We see that in the continuous limit, the energy of most of the configurations concentrate close to the energy of the macrostate p_M (see [Ellis et al., 2000, Potters et al., 2013] for a more precise discussion in the context of the 2D Euler equations). This is a consequence of the poloidal degrees of freedom mutually interacting through long range interactions. We can therefore enforce the constraint on the configuration energy as a macrostate constraint.

Following the argumentation yielding to (43) in the toroidal case, we conclude that in the limit of large N, the total poloidal entropy is equal to the poloidal entropy of the most probable poloidal macrostate which satisfies the constraints. Therefore,

$$S^{pol}(E, X_{tot}) = \sup_{p_M \in \mathcal{Q}^{pol}} \{\mathcal{S}^{pol}[p] \mid \mathcal{X}_{tot}[p_M] = X_{tot} \text{ and } \mathcal{E}_{pol}[p_M] = E\}. \tag{53}$$

The critical distributions $p_M^\star(\xi, \mathbf{x})$ of the poloidal macrostate entropy can be written in terms of two Lagrange multipliers $\beta_{pol}^{(M)}$ and $h^{(M)}$, respectively related to the constraints on the poloidal energy and on the poloidal circulation as

$$p_M^{\star,E}(\xi, \mathbf{x}) = \frac{1}{M Z_M^\star(\mathbf{x})} \exp\{\left(h^{(M)} - \frac{\beta_{pol}^{(M)} \psi(\mathbf{x})}{2}\right)\xi\},$$

$$\text{with} \quad Z_M^\star(\mathbf{x}) = \int_{-1}^{1} \mathrm{d}\xi \exp\{\left(h^{(M)} - \frac{\beta_{pol}^{(M)} \psi(\mathbf{x})}{2}\right) M\xi\}. \tag{54}$$

The Lagrange multipliers $h^{(M)}$ and $\beta_{pol}^{(M)}$ are defined through

$$X_{tot} = \int_{\mathcal{D}} \mathbf{dx} \, \frac{\partial \log Z_M^\star(\mathbf{x})}{\partial h^{(M)}} \text{ and } E = -\int_{\mathcal{D}} \mathbf{dx} \, \frac{\partial \log Z_M^\star(\mathbf{x})}{\partial \beta_{pol}^{(M)}}. \tag{55}$$

The moments of the one-point poloidal distribution can now be estimated from equation (54) as

$$\forall p \in \mathbb{N}, \langle \xi(\mathbf{x})^p \rangle_M^{pol,E} = \int_{-M}^{M} \mathrm{d}\xi \, p_M^\star(\xi, \mathbf{x}) \, \xi^p = \frac{\partial^p \log Z_M^\star(\mathbf{x})}{\partial h^{(M)p}}. \tag{56}$$

Taking $p = 1$ in equation (56) and using equation (51) yield the M-dependent self-consistent mean-field equation

$$\frac{\partial \log Z_M^\star(\mathbf{x})}{\partial h^{(M)}} = -\Delta^\star \psi. \tag{57}$$

We now need to let $M \to \infty$ to describe the microcanonical poloidal measure.

3.3.2 $M \to \infty$: Computation of the partial limit measures $<>^{pol,E}$

We suppose in this section that the energy is non zero. Otherwise $\psi \equiv 0$ and the equilibrium state is trivial.

Scaling of the Lagrange parameters In order for equation (55) to be satisfied whatever the value of M, the Lagrange multipliers need to be M-dependent. It seems reasonable to assume that $\beta^{(M)}$ and $h^{(M)}$ can be developped in powers of M when $M \to \infty$. If γ denotes the maximum between the leading orders of $\beta^{(M)}$ and $h^{(M)}$, so that $\beta_{pol}^{(M)} = M^\gamma \beta_{pol}^\star + o(M^\gamma)$, $h^{(M)} = M^\gamma h^\star + o(M^\gamma)$ and $(\beta^\star, h^\star) \neq (0,0)$, then necessarily $\gamma = -2$ (see Appendix A for a justification). One is therefore led to work with the reduced Lagrange multipliers

$$h^\star = \lim_{M\to\infty} M^2 h^{(M)}, \quad \text{and} \quad \beta^\star = \lim_{M\to\infty} \beta^{(M)}. \tag{58}$$

Mean-field equation and infinite temperature

Using the scaling (58) and letting $M \to \infty$ in equations (54) and (56) yield

$$\langle \xi(\mathbf{x}) \rangle = -\frac{\beta_{pol}^\star \psi(\mathbf{x})}{6} + \frac{h^\star}{3}, \quad \text{and} \quad \forall p > 1, \, |\langle \xi(\mathbf{x})^p \rangle| = \infty. \tag{59}$$

The limit mean-field equation stems from equation (59) combined with equation (57). It reads

$$\Delta^\star \psi = \frac{\beta_{pol}^\star \psi(\mathbf{x})}{6} - \frac{h^\star}{3}. \tag{60}$$

This equation is very reminiscent of the equation that describes the low energy equilibria or the strong mixing limit of the bidimensionnal Euler equations (see e.g. [Chavanis and Sommeria, 1998, Bouchet and Venaille, 2011]). It is thoroughly solved in appendix (B), and we qualitatively describe below its solutions.

The differential operator $-\Delta^\star$ is a positive definite operator. We denote by ϕ_{kl} and κ_{kl} the eigenfunctions and corresponding eigenvalues of $-\Delta^\star$, such that $\int_{\mathcal{D}} \mathbf{dx}\, \phi_{kl} \neq 0$. We denote ϕ'_{kl} and κ'_{kl} the eigenfunctions and corresponding eigenvalues such that $\int_{\mathcal{D}} \mathbf{dx}\, \phi'_{kl} = 0$. As shown in appendix B, three kinds of situations can be encountered for a solution ψ of (60).

- If $-\beta^\star/6$ is not one of the eigenvalue κ^2_{kl}, equation (60) has a unique solution $\psi(\beta^\star, h^\star)$, which is non-zero if $h^\star$ is non zero. If $h^\star \neq 0$, each $\psi(\beta^\star, h^\star)$ can be expressed as a sum of contributions on the modes ϕ_{kl} only. This family of solution is continuous for values of $-\beta^\star/6$ between two eigenvalues κ^2_{kl}, and diverge for $-\beta^\star/6$ close to κ^2_{kl}. In particular, it is continuous for $-\beta^\star/6 = \kappa'^2_{kl}$.

- If $\beta^\star = -6\kappa'^2_{k_0 l_0}$, ψ is the superposition of the eigenmode $\phi'_{k_0 l_0}$ with the solution from the continuum at temperature $\beta^\star = -6\kappa'^2_{k_0 l_0}$. In this case, we will say that ψ is a "mixed solution".

- If $\beta^\star = -6\kappa^2_{k_0 l_0}$, ψ is proportional to an eigenmode $\phi_{k_0 l_0}$.

Entropy and phase diagram All of the solutions described are critical points for the macrostate entropy. For given E and X_{tot} we selected among those critical points those that have the correct E and X_{tot}. If more than one solution exist, we select the ones that do indeed maximize the macrostate entropy. The computation of the entropy and the selection of the most probable states is carried out explicitly in appendix C.

The kind of solutions for which the macrostate entropy is maximal depends on the quantity $\dfrac{X^2_{tot}}{2E}$. We first define quantities necessary in order to describe the results. There exist two threshold values $T_- < T_+$ for this quantity, whose values can be found in appendix C. The value T_- depends on the geometry of the domain. It is close to T_+ for thin cylinders ($h \gg R$) and close to 0 (but not 0) for wide cylinders ($h \ll R$). We recall that κ^2_{01} is the minimal eigenvalue of the operator $-\Delta^\star$. We denote κ'^2 the minimal eigenvalue associated to the eigenfunctions ϕ'. Then $\kappa' = \kappa'_{02}$ for wide cylinders and $\kappa' = \kappa'_{11}$ for thin cylinders.

Then:

- For $\dfrac{X^2_{tot}}{2E} > T_+$, there is only one set of values ($\beta^\star$,$h^\star$) such that the critical points $\psi(\beta^\star, h^\star)$ satisfy the constraints on the energy and on the circulation. This is a solution from the continuum with $\beta^\star$ strictly greater than $-6\kappa^2_{01}$. This unique critical point is the entropy maximum. When $\dfrac{X^2_{tot}}{2E} \gg T_+$, the typical poloidal field is uniform. As $\dfrac{X^2_{tot}}{2E} \to T_+^+$, the typical poloidal field gets organized into a single large-scale vertical jet.

- For $\dfrac{X^2_{tot}}{2E} \in [T_-; T_+]$, the entropy is maximized for a solution from the continuum. The value of $h^\star$ and $\beta^\star$ are not uniquely determined by the value $\dfrac{X^2_{tot}}{2E}$ and the selected solution is the one that corresponds to $|\beta^\star| \leq 6\kappa'$. As $\dfrac{X^2_{tot}}{2E} \to T_-^+$, the vertical jet gets thinner.

- For $\dfrac{X^2_{tot}}{2E} \leq T_-$, the entropy is maximized by a mixed solution, associated to the

eigenvalue κ'. As $\frac{X_{tot}^2}{2E} \to 0$, the vertical jet gets transformed into a dipolar flow. The dipoles are vertical for wide cylinders and horizontal for thin cylinders.

Those results and the equilibrium poloidal fields $\langle \xi(\mathbf{x}) \rangle^{pol}$ are summarized on the phase diagram shown on Figure 4. Note that the entropy of the equilibrium state is

$$\mathcal{S}_M[p_M^{\star,E}] \underset{M\to\infty}{=} \log 2M + \frac{1}{2|\mathcal{D}|M^2}(\beta^\star E - h^\star X_{tot}) + o\left(\frac{1}{M^2}\right), \tag{61}$$

where for each energy the values of $\beta^\star$ and $h^\star$ are the ones described above.

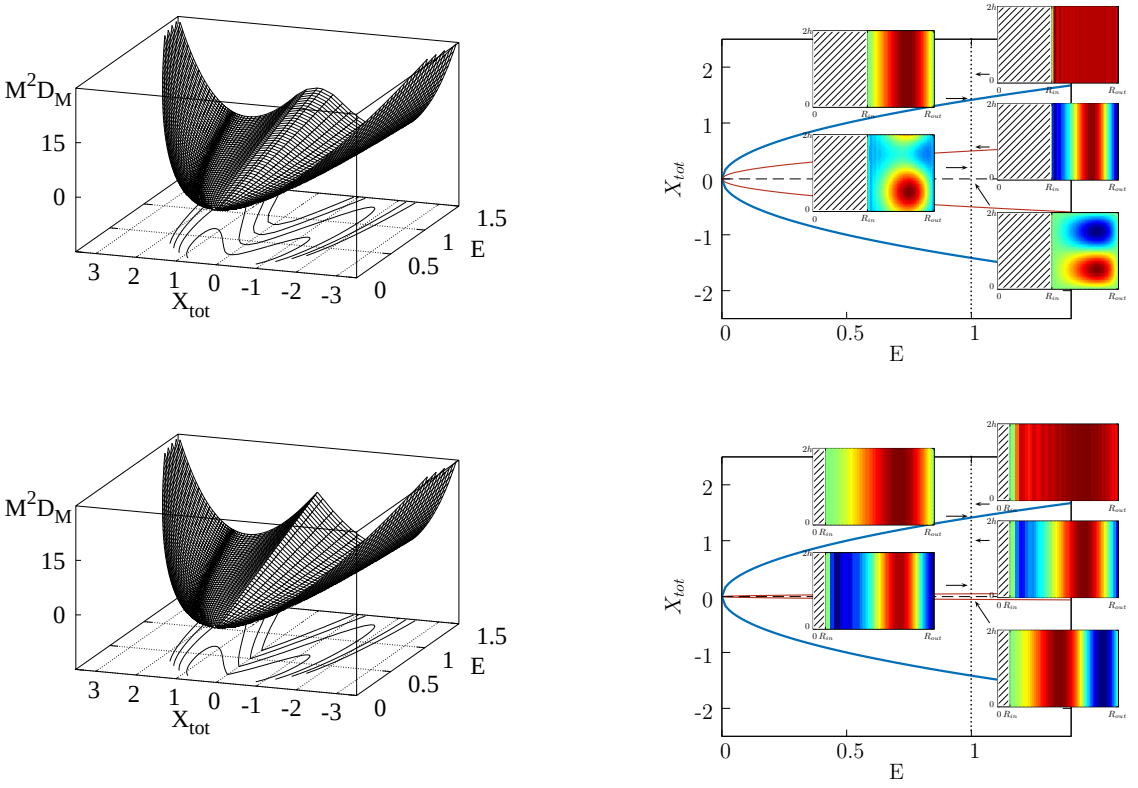

Figure 4: Left : Minus the poloidal entropy $M^2\mathcal{D}_M = 2|\mathcal{D}|M^2(\log 2M - \mathcal{S}_M)$ as a function of the circulation X_{tot} and of the poloidal energy E. The entropy was numerically estimated for a domain with height $2h = 1$, outer radius $R_{out} = \sqrt{2}$ and inner radius $R_{out} = 0.63$ (up) and $R_{in} = 0.14$ (down) . X_{tot} is rescaled by a factor $c_1 = \sqrt{\frac{|\mathcal{D}|}{32h}}$ and the entropy by a factor $c_2 = \left(\frac{|\mathcal{D}|}{2h\pi}\right)^2$ so that the value of T_+ is 1. Right: The corresponding poloidal phase diagrams. The typical poloidal fields $\langle \xi(\mathbf{x}) \rangle^{pol,E}$ are shown $E = 1$ and various values of X_{tot}. Those fields are renormalized by a factor $\sup_{\mathcal{D}} \left|\langle \xi(\mathbf{x}) \rangle^{pol,E}\right|$ so that the colormap ranks from -1 (blue) to 1 (red). With our choice of units the blue parabola has equation $X_{tot}^2 = 2E$. The red parabola separates the solutions from the continuum from the mixed solutions (see text and appendix C for details).

3.4 Statistical mechanics of the simplified problem

As explained in paragraph (3.1.3), we will now couple the toroidal and poloidal degrees of freedom in order to solve the simplified problem $\tilde{\mathcal{P}}$. The total entropy is then

$$S_M(E) = \sup_{E_{tor}} \{S_M^{pol}(E - E_{tor}) + S^{tor}(E_{tor})\}, \tag{62}$$

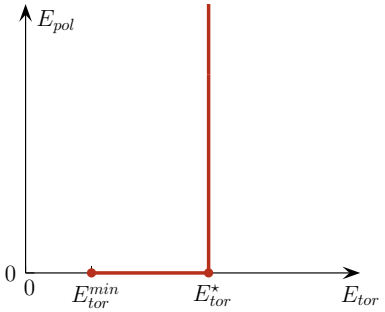

Figure 5: Phase diagram of problem $\tilde{\mathcal{P}}$.

where E_{tor} is the toroidal energy, $E - E_{tor}$ the poloidal one, the toroidal entropy S^{tor} is depicted in Figure 3, and the poloidal entropy is given by (61). The extrema condition leads to the equality of the poloidal and toroidal inverse temperatures

$$\beta_M^{pol} = \left.\frac{\partial S_M^{pol}(E_{pol}, X_{tot})}{\partial E_{pol}}\right|_{X_{tot}} = \beta^{tor} = \left.\frac{\partial S^{tor}(E_{tor}, \{A_k\})}{\partial E_{tor}})\right|_{\{A_k\}}. \tag{63}$$

The fundamental remark is that in the limit $M \to \infty$, because the number of poloidal degrees of freedom scales with M, the inverse poloidal temperature is equal to zero whenever the poloidal energy is non zero – see Eq. (61), and use that $\beta^\star \to \infty$ for $E_{pol} \to 0$. When the inverse poloidal temperature is zero, so is the inverse toroidal temperature. This prescribes that the toroidal energy reaches its extremal value $E^\star$ – see Figure 3. We are therefore left with two alternatives:

- $E < E^\star$ then $E_{pol} = 0$ and $E_{tor} = E$.
- $E > E^\star$ then $E_{pol} = E - E^\star$ and $E_{tor} = E^\star$.

The phase diagram corresponding to problem $\tilde{P}$ is then quite simple. It is shown on Figure 5, and we can describe the two kinds of equilibria it exhibits.

For small energies, ($e.g$ $E < E_{tor}^\star$), there is a large scale organization of the toroidal flow. In this region, the microcanonical temperature ${\beta_{tor}}^{-1}$ is positive. The smaller E is, the smaller the toroidal temperature is and the less the toroidal energy fluctuates. As for the poloidal flow, it is vanishing. In the case where X_{tot} is non-zero, the limit $E_{pol} \to 0$ exists but yields a singular distribution for the poloidal field, since it corresponds to a typical poloidal field having a non-zero momentum while having a vanishing energy.

For high energies, ($e.g$ $E > E_{tor}^\star$), the equilibria describe toroidal fields that are uniform, the levels of $\mathfrak{S}_K$ being completely intertwined. The poloidal fields have infinite fluctuations. This is a consequence of the microcanonical temperature being infinite. When the poloidal energy is small, typically $E_{pol} \ll \frac{1}{2}X_{tot}^2$, the typical poloidal field is uniform over the domain. For larger poloidal energies, the typical poloidal field gets organized into a single vertical jet ($E_{pol} \simeq \frac{1}{2}X_{tot}^2$) or a large-scale dipole ($E_{pol} \gg \frac{1}{2}X_{tot}^2$).

4 Statistical mechanics of the full problem

We now consider the full problem. It is quite straightforward to generalize the construction carried out for the simplified problem in order to build and compute a microcanonical

measure for the Euler axisymmetric equations. We find that the correlations play no role in selecting the equilibria, so that the phase diagram of the full problem is the same as the one found in the non-helical case. This is quite a striking result which is due to the temperature being infinite whenever the poloidal energy is non vanishing. As a result, the correlations average themselves out at every point of the domain, so that the coarse-grained equilibria only depend and on the circulation and on the total energy. The mathematical developments related to the full problem are presented in the next two subsections. The axisymmetric equilibria are described in (4.3).

4.1 Construction of the microcanonical measure

Unlike in the reduced problem $\tilde{\mathcal{P}}$, the poloidal and the toroidal fields are now coupled not only trough their respective energies, but also through the K partial circulations $\{X_k\}$. In this case, it is not very useful to introduce the toroidal and poloidal spaces of configurations. We therefore cut through this step and directly define the space of bounded Beltrami-spin configurations $\mathcal{G}_{M,N}(E,\{A_k\},\{X_k\})$ together with the phase space volume $\Omega_{M,N}(E,\{A_k\},\{X_k\})$ as

$$\begin{aligned}\mathcal{G}_{M,N}(E,\{A_k\},\{X_k\}) = \Big\{(\sigma_N,\xi_N)\in(\mathfrak{S}_K\times[-M;M])^{N^2} \;|\; \mathcal{E}\left(\sigma_N,\xi_N\right)=E \\ \text{and}\;\; \forall k\in[\![1;K]\!],\, \mathcal{A}_k\left[\sigma_N\right]=A_k \;\text{ and }\; \mathcal{X}_k\left[\sigma_N,\xi_N\right]=X_k\Big\}, \\ \text{and } \Omega_{M,N}(E,\{A_k\},\{X_k\}) = \sum_{\sigma_N\in\mathfrak{S}_K^{N^2}}\prod_{(i,j)\in[\![1;N]\!]^2}\int_{-\infty}^{+\infty}\mathrm{d}\xi_{N,ij}\mathbf{1}_{(\sigma_N,\xi_N)\in\mathcal{G}_{M,N}(E,\{A_k\},\{X_k\}}.\end{aligned} \tag{64}$$

It is then straightforward to generalize equations (19) and (21), and define the microcanonical weight $\mathrm{d}\mathcal{P}_{M,N}$ of a configuration $\mathcal{C}=(\sigma_N,\xi_N)\in\mathcal{G}_{M,N}(E,\{A_k\},\{X_k\})$, together with the M,N-dependent microcanonical averages $<>_{M,N}$. The microcanonical averages $<>_M$ and $<>$ are then defined by letting successively $N\to\infty$ and $M\to\infty$, accordingly to equation (22).

4.2 Estimate of $<>_M$ and $<>$ when $E_{pol}\neq 0$

Estimate of $<>_M$ We assume in the next two paragraphs that E_{pol} is prescribed and non negative. To obtain the limit $N\to\infty$ of the M,N dependent phase space volume, we follow the steps described in paragraphs (3.2) and (3.3) in order to write $\Omega_{M,N}(E,\{A_k\},\{X_k\})$ in terms of a macrostate entropy provided by Sanov theorem.

Randomly and independently assigning on each node of the lattice a random value of ξ from the uniform distribution over the interval $[-M;M]$ together with a random value of σ_k drawn from the uniform distribution over $\mathfrak{S}_K$, we then define through a coarse-graining procedure the local probability $p_{k,M}\left(\xi,\mathbf{x}\right)$ that a Beltrami spin takes a toroidal value σ_k together with a poloidal value between ξ and $\xi+\mathrm{d}\xi$ in an infinitesimal area $\mathbf{dx}$ around a point $(\mathbf{x})$. The distributions $p_M=\{p_{k,M}(\xi,\cdot)\}_{\substack{k\in[\![1;K]\!]\\ \xi\in[-M;M]}}$ define a poloidal macrostate, which satisfies the local normalization constraint :

$$\forall\mathbf{x}\;\in\mathcal{D},\sum_{k=1}^{K}\int_{-M}^{M}\mathrm{d}\xi\, p_{k,M}\left(\xi,\mathbf{x}\right)=1. \tag{65}$$

We denote $\mathcal{Q}$ the sets of all the macrostates. The macrostate entropy is then given by

$$\mathcal{S}_M[p_M] = -\frac{1}{|\mathcal{D}|}\int_{\mathcal{D}} \mathbf{dx} \sum_{k=1}^{K} \int_{-M}^{M} \mathrm{d}\xi \, p_{k,M}(\xi, \mathbf{x}) \log p_M(\xi, \mathbf{x}), \tag{66}$$

and the constraints for the configurations of Beltrami spins can be related to constraints for the macrostates as

$$\begin{aligned} &\mathcal{A}_k[p_M] = \int_{\mathcal{D}} \mathbf{dx} \int_{-M}^{M} \mathrm{d}\xi \, p_{k,M}(\xi, \mathbf{x}), \quad \mathcal{X}_k[p_M] = \int_{\mathcal{D}} \mathbf{dx} \int_{-M}^{M} \mathrm{d}\xi \, \xi p_{k,M}(\xi, \mathbf{x}), \\ &\text{and } \mathcal{E}[p_M] = \frac{1}{2}\int_{\mathcal{D}} \mathbf{dx} \sum_{k=1}^{K} \int_{-M}^{M} \mathrm{d}\xi \, \{\frac{\sigma_k^2}{2y} + \psi(\mathbf{x})\,\xi\} p_{k,M}(\xi, \mathbf{x}). \end{aligned} \tag{67}$$

Then, the total entropy is given by the entropy of the most probable poloidal macrostate which satisfies the constraints. Therefore,

$$\begin{aligned} S(E, \{A_k\}, \{X_k\}) = \sup_{p_M \in \mathcal{Q}} \{\mathcal{S}_M[p_M] \mid \forall k \in [\![1; K]\!] \; \mathcal{A}_k[p_M] = A_k, \\ \mathcal{X}_k[p_M] = X_k \text{ and } \mathcal{E}[p_M] = E\}. \end{aligned} \tag{68}$$

The critical distributions $p_M^\star(\xi, \mathbf{x})$ of the optimization problem (68) can be written using $2K+1$ Lagrange multipliers as

$$\begin{aligned} &p_{M,k}^\star(\xi, \mathbf{x}) = \frac{1}{M Z_M^\star(\mathbf{x})} \exp\{\alpha_k^{(M)} - \frac{\beta^{(M)}\sigma_k^2}{4y} + \left(h_k^{(M)} - \frac{\beta^{(M)}\psi(\mathbf{x})}{2}\right)\xi\}, \\ &\text{with } \; Z_M^\star(\mathbf{x}) = \sum_{k=1}^{K} \int_{-1}^{1} d\xi \exp\{\alpha_k^{(M)} - \frac{\beta^{(M)}\sigma_k^2}{4y} + \left(h_k^{(M)} - \frac{\beta^{(M)}\psi(\mathbf{x})}{2}\right) M\xi\}, \end{aligned} \tag{69}$$

where the Lagrange multipliers $\alpha_k^{(M)}$, $h_k^{(M)}$, $\beta^{(M)}$ are determined through

$$\begin{aligned} A_k = \int_{\mathcal{D}} \mathbf{dx} \frac{\partial \log Z_M^\star(\mathbf{x})}{\partial \alpha_k^{(M)}}, \; X_k = \int_{\mathcal{D}} \mathbf{dx} \frac{\partial \log Z_M^\star(\mathbf{x})}{\partial h_k^{(M)}}, \\ \text{and } E = -\int_{\mathcal{D}} \mathbf{dx} \frac{\partial \log Z_M^\star(\mathbf{x})}{\partial \beta^{(M)}}. \end{aligned} \tag{70}$$

From (70), we can compute the one-point moments as

$$\langle \sigma^p(\mathbf{x}) \rangle_M = \sum_{k=1}^{K} \int_{-M}^{M} \mathrm{d}\xi \, \sigma_k^p \, p_{M,k}^\star(\xi, \mathbf{x}) \text{ and } \langle \xi^p(\mathbf{x}) \rangle_M = \sum_{k=1}^{K} \int_{-M}^{M} \mathrm{d}\xi \, \xi^p p_{M,k}^\star(\xi, \mathbf{x}). \tag{71}$$

In particular, the stream function solves

$$\Delta^\star \psi(\mathbf{x}) = -\langle \xi(\mathbf{x}) \rangle_M = -\sum_{k=1}^{K} \frac{\partial \log Z_M^\star(\mathbf{x})}{\partial h_k^{(M)}}. \tag{72}$$

Finally, note that the average one-point helicities read :

$$\langle \sigma(\mathbf{x})\, \xi(\mathbf{x}) \rangle_M = \sum_{k=1}^{K} \int_{-M}^{M} \mathrm{d}\xi \, \xi \sigma_k \, p_{M,k}^\star(\xi, \mathbf{x}). \tag{73}$$

Estimate of <> and mean-field closure equation In order to take the limit $M \to \infty$ in (71) and (72), one has to specify a scaling for the Lagrange parameters, as done in the purely poloidal case. Generalizing the argument exposed in Appendix A, one is led to define the following reduced Lagrange multipliers

$$\alpha_k = \lim_{M\to\infty} M^0 \alpha_k^{(M)}, \quad h_k^\star = \lim_{M\to\infty} M^2 h_k^{(M)}, \quad \text{and} \quad \beta^\star = \lim_{M\to\infty} M^2 \beta^{(M)}. \tag{74}$$

Using the scalings (74) to take the limit $M \to \infty$ in (72) and (71), one readily obtains

$$\forall p \geq 1 \, \langle \sigma^p(\mathbf{x}) \rangle = \overline{\sigma_k^p}\,, \tag{75}$$

$$\text{together with} \quad \langle \xi(\mathbf{x}) \rangle = -\frac{\beta^\star}{6}\psi(\mathbf{x}) + \frac{1}{3}\overline{h_k^\star}, \quad \text{and} \quad \forall p \geq 2 \; |\langle \xi^p(\mathbf{x}) \rangle| = +\infty, \tag{76}$$

where for any $\{\mathcal{O}_k\}_{1\leq k\leq K}$, $\overline{\mathcal{O}_k}$ is defined by $\overline{\mathcal{O}_k} \equiv \sum_{k=1}^K \frac{A_k}{|\mathcal{D}|}\mathcal{O}_k$.

The equilibrium streamfunction then solves

$$\Delta^\star \psi = \frac{\beta^\star}{6}\psi - \frac{1}{3}\overline{h_k^\star}, \tag{77}$$

which is very similar to equation describing ψ in the purely poloidal problem (60).

The one-point helicities (73) read

$$\langle \sigma(\mathbf{x})\, \xi(\mathbf{x}) \rangle = \frac{\overline{\sigma_k h_k^\star}}{6} + \langle \sigma(\mathbf{x}) \rangle \langle \xi(\mathbf{x}) \rangle. \tag{78}$$

Hence, the toroidal and the poloidal fields remain correlated in the limit $M \to \infty$. They first term of the r.h.s can be interpreted as an extra small-scale contribution to the total helicity.

The critical points of the macrostate entropy (66) are not necessarily maximizers of the macrostate entropy, and we still need to determine the values of $\overline{h_k^\star}$ and $\beta^\star$ that actually solve the optimization problem (71) for large values of M. To do so, we compute an asymptotic expansion of the critical values of the macrostate entropy. The computation is explained in Appendix D. We obtain

$$\begin{aligned} \mathcal{S}_M[p_M^\star] \underset{M\to\infty}{=} \log 2M - \sum_{k=1}^K \frac{A_k}{|\mathcal{D}|} \log \frac{A_k}{|\mathcal{D}|} + \frac{1}{2\,|\mathcal{D}|\,M^2}\left(\beta^\star E_{pol} - \overline{h_k^\star} X_{tot}\right) \\ + \frac{3}{2M^2}\overline{\left(\frac{X_k}{A_k} - \frac{X_{tot}}{|\mathcal{D}|}\right)^2} + o\left(\frac{1}{M^2}\right). \end{aligned} \tag{79}$$

This expression compares with the poloidal macrostate entropy (61) computed in the reduced problem. We conclude that the selection of the most poloidal probable state only depends on the value of E_{pol} and X_{tot}. For a given value of E_{pol} the selected macrostates are the same in the poloidal simplified problem and in the full problem.

4.3 Phase diagram of the full problem

In last section, we have obtained in formula (75) that the levels σ_k are completely mixed. As a consequence, $E_{tor} = E^\star$. In order to get this result, we have assumed that $\psi \neq 0$ or equivalently $E_{pol} \neq 0$. We thus deduce the same alternative as in the reduced problem:

- If $E \geq E^\star_{tor}$, then $E_{tor} = E^\star_{tor}$ and $E_{pol} = E - E^\star_{tor}$.
- If $E < E^\star_{tor}$, then $E_{tor} = E$ and $E_{pol} = 0$.

$E^\star_{tor}$ is computed from (75) as $E^\star_{tor} = \sum_{k=1}^{K} \frac{A_k \sigma_k^2}{2\,|\mathcal{D}|} \log \frac{R_{out}}{R_{in}}$. Therefore, the phase diagram describing how the total energy is dispatched between the toroidal and the poloidal degrees of freedom is the same as the one described for the simplified problem and corresponds to Figure 5. Hence, the axisymmetric equilibria are akin to the equilibria described in paragraph (3.4) for the non-helical problem and are of two different kinds.

Positive temperature, low energy equilibria When $E \leq E^{tor}_\star$, the poloidal energy is zero. Therefore, the stream-function is uniformly zero. $h_k^{(M)} \to 0$ as $M \to \infty$, so that to second order in M, the partition function $Z^\star_M$ of equation (69) is exactly the toroidal partition function given by equation (45). From this observation, we conclude that there is no difference between the low energy equilibria of the simplified problem and the low energy equilibria of the full problem. The toroidal flow is organized in vertical stripes, whose boundaries fluctuate more and more as the energy gets close to $E^\star_{tor}$. The poloidal flow is vanishing. In the limit where E is infinitely close to $E^\star_{tor}$, the microcanonical temperature becomes infinitely large, yielding the toroidal stripes to vanish.

Infinite temperature, high energy equilibria When $E \geq E^{tor}_\star$, the poloidal energy is prescribed $E_{pol} = E - E^\star_{tor}$. The toroidal field is uniform, correspondind to the levels of $\mathfrak{S}_K$ being completely intertwined, regardless of the position in the domain $\mathcal{D}$. The poloidal field exhibits infinitely large fluctuations around a large scale organization. For prescribed values of the constraints, the entropy of the full problem (79) is the one of the poloidal problem (61) up to some constants terms. Hence, the large scale organization of the poloidal field is exactly the one summarized on Figure 4.

4.4 Link to previous work.

We have argued that the limit $M \to \infty$ is required to describe microcanonical measures for the axisymmetric Euler equations. In this limit, the typical fields (76) satisfy some relations that are very different from the relations found in previous works [Leprovost et al., 2006,Naso et al., 2010a]. In those papers it is found that the typical fields correspond to Beltrami flows, such that $\langle \sigma(\mathbf{x}) \rangle = B\psi(\mathbf{x})$ and $\langle \xi(\mathbf{x}) \rangle = B\langle \sigma \rangle / 2y + C$, where B and C are related to the Lagrange multipliers associated to the constraints of energy, helicity and angular momentum – see for example equations (36) and (37) of [Naso et al., 2010a]. There are two reasons for this difference : (i) in the previous papers only three invariants are taken into account, and (ii) (more importantly) no fluctuations on the poloidal field are considered.

We can however retrieve this limit of vanishing fluctuations with our approach. No fluctuations on the poloidal field means that not only the areas A_k and partials circulations $X_k = \mathcal{X}_k[\sigma, \xi] = \int_{\mathcal{D}} \mathbf{dx}\, \xi \mathbf{1}_{\sigma(\mathbf{x})=\sigma_k}$ are prescribed but also the partial moments $\mathcal{W}_{p,k}[\sigma, \xi] = \int_{\mathcal{D}} \mathbf{dx}\, \xi^p \mathbf{1}_{\sigma(\mathbf{x})=\sigma_k}$. In such a toy model, each Beltrami spin has a "frozen" poloidal degree of freedom. Hence, the toroidal degrees of freedom mutually interact trough the long range correlations between the poloidal degrees of freedom, which makes the situation very similar to the 2D case.It is straightforward to see that in the simple case where we consider only two symmetric levels for the toroidal degrees of freedom (say -1 and +1),

the typical toroidal field and poloidal field both satisfy sinh- Poisson like relations, namely :

$$\begin{aligned} \langle \sigma(\mathbf{x}) \rangle &= \tanh \frac{1}{2} \left[A + B\psi(\mathbf{x}) \right], \\ \text{and } \langle \xi(\mathbf{x}) \rangle &= \frac{\dfrac{X_+}{A_+} e^{\dfrac{A + B\psi(\mathbf{x})}{2}} + \dfrac{X_-}{A_-} e^{-\dfrac{A + B\psi(\mathbf{x})}{2}}}{2 \cosh \dfrac{1}{2} \left[A + B\psi(\mathbf{x}) \right]}. \end{aligned} \tag{80}$$

where A and B are functions of the Lagrange multipliers and hence functions of the A_k and the energy E. In the limit of a vanishing stream function, one retrieves an affine relationship both between the toroidal field and the stream function and between the poloidal field and the stream function, akin to the Beltrami states of [Leprovost et al., 2006].

Those "quenched" axisymmetric measures can therefore be thought of seen as a bridge between 2D-like axisymmetric measures and the axisymmetric measures described in this paper. Let us once again emphasize, that there is no physical reason for this quench.

5 Discussion

Technical comments It was not so obvious from the beginning that the construction of microcanonical measures *à la* Robert-Miller-Sommeria for the axisymmetric Euler equations could be carried out extensively, nor that it would yield non trivial insights to understand the physics of axisymmetric flows. What can be considered as the key point here is the accurate renormalization of the inverse temperature and associated Lagrange multipliers with respect to the phase space volume. This allowed us to build an asymptotic limit consistent with the physical constraints and prevented us from encountering an avatar of the Jeans paradox. The renormalization was not carried out in the previous works concerning axisymmetric equilibria. Here, it is crucial in order to take into account the invariants related to the poloidal degrees of freedom that live in an infinite phase space. Other choices could have been made to renormalize the phase space. Instead of a cutoff M, it is also possible to make the divergent integrals converge by integrating over the ν dependent measures $e^{-\nu\xi^2}\mathrm{d}\xi$ – rather than over the M dependent measures $\mathbf{1}_{[-M;M]}\mathrm{d}\xi$ – , introduce the ν dependent Lagrange multipliers $\beta^\nu = \nu\beta^\star$, $h^\nu = \nu h^\star$ and let $\nu \to 0$ subsequently. The limit measures obtained with the latter renormalization are consistent with the ones we described in this paper.

Note also that in order to carry out our analysis, we restricted ourselves to the case where the inner cylinder has a non-vanishing radius R_{in}, so that we worked in the framework of a "Tayor-Couette geometry". It is yet not so clear how to extend the analysis to the limit case $R_{in} \to 0$ corresponding to a "von Kármán geometry". The problem comes from the blow up of the equilibrium toroidal energy $E^\star_{tor} = \sum_{k=1}^K \dfrac{A_k \sigma_k^2}{2\left|\mathcal{D}\right|} \log \dfrac{R_{out}}{R_{in}}$ if we simply let $R_{in} \to 0$. [3]

[3] One naive way to cope with this issue and obtain a specific class of equilibria for the von Kármán geometry is to renormalize each toroidal level σ_k^2 in $\mathfrak{S}_K$ as $\sigma_k^2 \to \dfrac{\sigma_k^2}{\log \dfrac{R_{out}}{R_{in}}}$. Another possibility is to

Physical insights about axisymmetric turbulence

The physics described by the micrononical measure is interesting. Let us first comment about the role of the invariants. We may have built a measure by taking into account every kind of inviscid invariant of the axisymmetric Euler equations, it turns out that most of the physics comes from a reduced set of invariants, namely the energy, the toroidal Casimirs and the total circulation. In particular, our result shows that the helicity – which relates to the correlation between the toroidal and the poloidal degrees of freedom – plays no role in the description of large scale structure at the level of the macrostates. This is consistent with the traditionnal picture of a downward helicity cascade in $3D$ turbulence. This may also explain why previous attempts to find axisymmetric equilibria [Leprovost et al., 2006, Naso et al., 2010a] by neglecting the fluctuations of the poloidal field while keeping a constraint on the helicity would only lead to unstable equilibria, likely to be destabilized by small-scaled perturbations.

The axisymmetric equilibria are very different from those obtained in the 2D case. In the low temperature, low energy regime, the large scale stripes come from the interaction of the toroidal degrees of freedom with the position field – the interaction being inhomogeneous and invariant with respect to vertical translations. As for the infinite temperature, high energy regime, the toroidal Casimirs play no role in it. The linear relationship between the poloidal field and the stream function may be seen as the axisymmetric ananalogue of the low energy limit of the sinh-Poisson relation in 2D turbulence. Yet, the infinite fluctuations related to the poloidal field may be heuristically interpreted as a very 3D turbulent feature and may be related to the tendency of vortices to leak towards the smallest scales available in 3D turbulence. Therefore, neither regimes have strict analogues in 2D.

Perspectives.

Are microcanical measures relevant for real turbulence ? It is tempting to ask wether some of the axisymmetric equilibrium features can be recognized in real turbulent experiments. An example of a turbulent flow likely to be modelized by the axisymmetric Navier-Stokes is von Kármán turbulence [Herbert et al., 2012, Saint-Michel et al., 2013]. Using the Particle Image Velocity (PIV) technique, it is possible to investigate the properties of the large scale structures –if any– in such turbulent configurations. Preliminary results tend to show a connection between the $M = 0$ scenario and some turbulent stationnary states in a von Kármán axisymmetric geometry. There exist many caveats concerning a thorough investigation of the link between the axisymmetric measures and turbulent experiments. We therefore postpone the discussion to a forthcoming paper.

Extensions to closely related flows. Finally, let us mention the close analogy between axisymmetric flows and other flows of geophysical and astrophysical interests such as two-dimensional stratified flows in the Boussinesq approximation (Boussinesq flows) [Szeri and Holmes, 1988, Abarbanel et al., 1986] and two-dimensional magnetohydrodynamics (2D MHD). In the former case, it almost suffices to replace the word "poloidal" by the word "vorticity" and the word "toroidal" by the word "density " in the present paper

impose a local smoothing condition near the center of the cylinder that could be enforced at the level of the macrostates. It would suffice for instance to prescribe $< \sigma(\mathbf{x}) >_M \underset{r\to 0}{=} O(r^\epsilon)$ with ϵ being non negative in order to avoid a blow up of the equilibrium toroidal energy.

to obtain *mutatis mutandi* a statistical theory for ideal Boussineq flows. The case of 2D MHD is slightly more subtle. The Casimir invariants of ideal 2D MHD are similar to the axisymmetric Casimir invariants [Weichman, 2012] but the energies slightly differ. It would therefore be very interesting to generalize the method described in the present paper to the 2D MHD case, which is more documented than the axisymmetric case, and for which invicid statistical theories have recently been reinvestigated [Weichman, 2012].

A Scaling of the Lagrange multipliers to compute the poloidal partial measures

We suppose that the energy is non zero and finite. We show that in order to enforce the constraint on the energy as $M \to \infty$, the Lagrange multipliers $\beta_{pol}^{(M)}$ and $h^{(M)}$ have to scale as $\dfrac{1}{M^2}$.

Let γ be a yet unprescribed parameter, and let us define

$$\beta^\star = \lim_{M\to\infty} M^{-\gamma}\beta_{pol}^{(M)} \text{ and } h^\star = \lim_{M\to\infty} M^{-\gamma}h^{(M)}. \tag{81}$$

Let us now consider a fluid element in the vicinity of a point $(\mathbf{x_0})$ where the quantity $f_0^\star = h^\star - \frac{1}{2}\beta^\star\psi\left(\mathbf{x_0}\right)$ is non zero – this point exists otherwise the stream function ψ would be constant over the domain $\mathcal{D}$ and the poloidal energy would be zero. ψ being continuous in the limit $N \to \infty$, we may assume $\psi\left(\mathbf{x_0}\right) > 0$ on a small volume of fluid $|\mathbf{dx_0}|$ centered around $(\mathbf{x_0})$. To leading order in M, this small volume of fluid contributes to the poloidal energy as

$$E\left(\mathbf{x_0}\right)|\mathbf{dx_0}| = -\frac{\partial \log Z_M^\star\left(\mathbf{x_0}\right)}{\partial\beta_{pol}^{(M)}}|\mathbf{dx_0}| = \frac{M\psi\left(\mathbf{x_0}\right)|\mathbf{dx_0}|}{2}\frac{\int_{-1}^{1} d\xi\xi e^{f_0^\star M^{\gamma+1}\xi}}{\int_{-1}^{1} d\xi e^{f_0^\star M^{\gamma+1}\xi}}. \tag{82}$$

If $\gamma + 1 \geq 0$ then $E\left(\mathbf{x_0}\right)|\mathbf{dx_0}| \to \infty$, and the divergence is exponential when $\gamma > 1$. Therefore, necessarily $\gamma + 1 \leq 0$. In that case $E\left(\mathbf{x_0}\right)|\mathbf{dx_0}| \underset{M\to\infty}{\sim} \dfrac{M^{\gamma+2}\psi\left(\mathbf{x_0}\right)f_0^\star}{12}|\mathbf{dx_0}|$ which is finite and non zero only when $\gamma = -2$.

B Solutions of the mean-field equation

We show here how to solve the closure equations (60) and (77) for fields that are $2h$-periodic along the z direction and are vanishing on both of the walls of the cylinder. Those two equations can be written as

$$\Delta^\star\psi = \frac{\beta^\star}{6}\psi - \frac{h^\star}{3} \quad \text{with} \quad \Delta^\star = \frac{1}{2y}\partial_{zz} + \partial_{yy}. \tag{83}$$

We will solve those equations in terms of the eigenmodes of the operator $\Delta^\star$ with periodic conditions along the z direction and vanishing boundary conditions on both walls.

B.1 Explicit computation of the eigenmodes of the operator $\Delta^\star$

The eigenmodes of $\Delta^\star$ correspond to the solutions of the eigenvalue problem $\Delta^\star\phi_\kappa = -\kappa^2\phi_\kappa$ with the prescribed boundary conditions. Let ϕ_κ be such an eigenmode. We can Fourier decompose ϕ_K and write $\phi_K(y,z) = \sum_{k\in\mathbb{Z}} f_k(y)\exp\dfrac{ik\pi z}{h}$. ϕ_K is a solution to the eigenvalue probleme *iff* each one of the functions f_k satisfies

$$f_k''(y) + \left(\kappa^2 - \frac{k^2\pi^2}{2h^2 y}\right)f_k(y) = 0, \tag{84}$$

$$\text{or equivalently } \tilde{f}_k''(\tilde{y}) + \left(1 - \frac{k^2\pi^2}{2h^2\kappa\tilde{y}}\right)\tilde{f}_k(\tilde{y}) = 0 \text{ putting } \tilde{y} = \kappa y \text{ and } \tilde{f}_k(\tilde{y}) = f_k(y). \tag{85}$$

Equation (85) is an equation known as a "Coulomb Wave equation".

If $k = 0$, then $f_0(y) = A \sin \kappa (y - Y_{in}) + B \cos \kappa (y - Y_{in})$. $f_0(Y_{in}) = 0$ gives $B = 0$. $f_0(Y_{out}) = 0$ gives $\kappa = \kappa_{0l} = \dfrac{l\pi}{Y_{out} - Y_{in}}$. For each value of $l \geq 0$, we write $\phi_{0l} = \dfrac{\sin\left[\kappa_{0l}\left(y - Y_{in}\right)\right]}{\sqrt{h(Y_{out} - Y_{in})}}$. ϕ_{0l} is an eigenmode of $\Delta^\star$ so that $\Delta^\star \phi_{0l} = -\kappa_{0l}^2 \phi_{0l}$. The normalization factor is chosen so that $\displaystyle\int_{Y_{in}}^{Y_{out}} dy \int_0^{2h} dz \phi_{0l}^2 = 1$.

If $k \neq 0$, $\tilde{f}_k(\tilde{y}) = C_1 F_0\left(\eta_k, \tilde{y}\right) + C_2 G_0\left(\eta_k, \tilde{y}\right)$ where F_0 and G_0 are respectively the regular and singular Coulomb Wave functions associated to the parameter $\eta_k = \dfrac{k^2\pi^2}{4h^2\kappa}$. The non trivial solutions are determined using the vanishing boundary conditions on the walls. For each value of k, the horizontal modes correspond to the values κ_{kl} for wich the quantity

$$W(\kappa) = \begin{vmatrix} F_0\left(\dfrac{k^2\pi^2}{4h^2\kappa}, \kappa Y_{in}\right) & G_0\left(\dfrac{k^2\pi^2}{4h^2\kappa}, \kappa Y_{in}\right) \\ F_0\left(\dfrac{k^2\pi^2}{4h^2\kappa}, \kappa Y_{out}\right) & G_0\left(\dfrac{k^2\pi^2}{4h^2\kappa}, \kappa Y_{out}\right) \end{vmatrix} \text{ is vanishing.} \tag{86}$$

Each mode κ_{kl} is therefore related to two eigenmodes $\phi_{kl}^{\pm} = A_{kl} \exp\left(\pm i \dfrac{k\pi z}{h}\right) f_k(\kappa_{kl} y)$, such that $\Delta^\star \phi_{kl} = -\kappa_{kl}^2 \phi_{kl}$. The normalization factor is chosen so that $\displaystyle\int_{Y_{in}}^{Y_{out}} dy \int_0^{2h} dz \phi_{Kl}^2 = 1$.

The Fourier decomposition of ϕ_K can now be rewritten as $\phi_K(y, z) = \displaystyle\sum_{k,l \in \mathbb{Z}} a_{kl} \phi_{kl}(y, z)$. Two modes corresponding to two different eigenvalues are orthogonal for the scalar product $(f|g) \equiv \displaystyle\int_{\mathcal{D}} dy dz \bar{f} g$. Hence, ϕ_K is a solution of $\Delta^\star \psi = -\kappa^2 \phi_K$ *iff* there exists (k, l) such that $\kappa_{kl}^2 = \kappa^2$.

As an illustration, a numerical estimation for different domain shapes of the first eigenvalues of $\Delta^\star$ together with their corresponding eigenmode is provided on Figure 6.

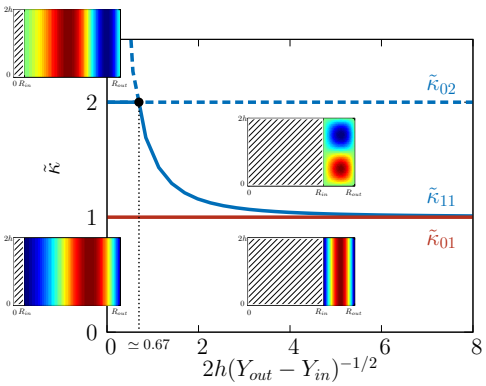

Figure 6: Numerical estimation of the first eigenvalues of $\Delta^\star$ as functions of the domain size. The eigenvalues κ are adimensionnalised and $\tilde{\kappa} = \dfrac{\kappa}{\pi(Y_{out} - Y_{in})}$. The estimation was made with a fixed height $2h = 1$ and fixed outer radius $R_{out} = \sqrt{2}$. The inserted pictures represent maps of the corresponding eigenmodes.

B.2 Types of solutions for equation (83).

Let ψ be a solution of equation (83) and let us decompose ψ as $\psi = \sum_{k,l} p_{kl}\phi_{kl}$.

Then necessarily,

$$\forall (k,l) \in \mathbb{Z}^2 \quad p_{kl}\left(\kappa_{kl}^2 + \frac{\beta^\star}{6}\right) = \frac{h^\star}{3}(1|\phi_{kl}). \tag{87}$$

Let us note that the only modes with a non vanishing integral over the domain, –e.g such that $(1|\phi_{kl}) \neq 0$ – are the modes obtained for $k = 0$ and l odd. To describe the solutions of equation (87) we need to consider the three following different cases.

Solutions from the continuum If $\forall (k,l), \beta^\star \neq -6\kappa_{kl}^2$, then necessarily

$$\forall (k,l) \;\; p_{kl} = \frac{h^\star (1|\phi_{kl})}{3\left(\kappa_{kl}^2 + \frac{\beta^\star}{6}\right)}. \tag{88}$$

In this case, ψ can be written as

$$\psi = \frac{h^\star}{3}\sum_{k,l} \frac{(1|\phi_{kl})}{\left(\kappa_{kl}^2 + \frac{\beta^\star}{6}\right)}\phi_{kl} = \frac{h^\star}{3}\sum_{l\, odd} \frac{(1|\phi_{0l})}{\left(\kappa_{0l}^2 + \frac{\beta^\star}{6}\right)}\phi_{0l} \tag{89}$$

For any odd value of l, this family of solution is continuous for values of $-\beta^\star/6$ between two eigenvalues κ_{0l}^2 and κ_{0l+2}^2 , and diverge for $-\beta^\star/6$ close to κ_{0l}^2. In particular, it is continuous for values of $-\beta^\star/6 = \kappa_{mn}^2$ such that $(1|\phi_{mn}) = 0$. Following the terminology of [Naso et al., 2010b], we therefore refer to those solutions as solutions "from the continuum".

Mixed solutions and eigenmodes Otherwise there exists (k_0, l_0) such that $\beta^\star = -6\kappa_{k_0 l_0}^2$. Then necessarily $\forall (k,l) \neq (k_0,l_0) \;\; p_{kl} = \frac{h^\star (1|\phi_{kl})}{3\left(\kappa_{kl}^2 - \kappa_{0l_0}^2\right)}$.

- Mixed Solutions. If $(1|\phi_{k_0 l_0}) = 0$, – *e.g* if $k_0 \neq 0$ or l_0 is even –, then ψ can be written as $\psi = p_{k_0 l_0}\phi_{k_0 l_0} + \frac{h^\star}{3}\sum_{l\, odd} \frac{(1|\phi_{0l})}{\left(\kappa_{0l}^2 - \kappa_{k_0 l_0}^2\right)}\phi_{0l}$. The coefficient $p_{k_0 l_0}$ can take any value. ψ can be seen as a superposition of a solution from the continuum with the eigenmode $\phi_{k_0 l_0}$, and we therefore call these solutions "mixed solutions".
- Odd eigenmodes. Otherwise, $(1|\phi_{k_0 l_0}) \neq 0$ – *e.g* $k_0 = 0$ and l_0 is odd. Equation (87) considered for $(k,l) = (0, l_0)$ implies $h^\star = 0$. In this case ψ is proportionnal to the odd eigenmode ϕ_{0l_0}, namely $\psi = A\phi_{0l_0}$.

C Maximizers of the macrostate entropy for the simplified poloidal problem.

The constraints E and X_{tot} being given, we want to determine the values of $h^\star$ and $\beta^\star$ that minimize the poloidal macrostate entropy (48).

C.1 Computation of the macrostrate entropy for the critical distributions $p_M^{\star,E}$.

The critical distributions $p_M^{\star,E}$ are described by equations (54) and (55). Their macrostate entropy reads

$$\begin{aligned}\mathcal{S}_M^{pol}[p_M^{\star,E}] &= -\frac{1}{|\mathcal{D}|}\int_{\mathcal{D}}\mathbf{dx}\int_{-M}^{M}\mathrm{d}\xi\, p_M^{\star,E}(\xi,\mathbf{x})\log p_M^{\star,E}(\xi,\mathbf{x})\\ &= -\frac{1}{|\mathcal{D}|}\int_{\mathcal{D}}\mathbf{dx}\int_{-M}^{M}d\xi\, p_M^{\star,E}(\xi,\mathbf{x})\left\{\left(h^{(M)}-\beta^{(M)}\frac{\psi(\mathbf{x})}{2}\right)\xi-\log M-\log Z_M^{\star}(\mathbf{x})\right\}\\ &= \log M-\frac{1}{|\mathcal{D}|}\left(h^{(M)}X_{tot}-\beta^{(M)}E\right)+\frac{1}{|\mathcal{D}|}\int_{\mathcal{D}}\log Z_M^{\star}(\mathbf{x})\,. \end{aligned}\tag{90}$$

The last equality is obtained using $\int_{-M}^{M}\mathrm{d}\,\xi\, p_M^{\star,E}(\xi,\mathbf{x})=1$ on one hand, and remembering that

$$\int_{\mathcal{D}}\mathbf{dx}\int_{-M}^{M}\mathrm{d}\xi\, p_M^{\star,E}(\xi,\mathbf{x})=X_{tot} \text{ and } \int_{\mathcal{D}}\mathbf{dx}\int_{-M}^{M}\mathrm{d}\xi\,\frac{\psi}{2}\xi\, p_M^{\star,E}(\xi,\mathbf{x})=E \text{ on the other hand.}$$

The asymptotic development of $\log Z_M^{\star}(\mathbf{x})$ for large M yields

$$\begin{aligned}\log Z_M^{\star}(\mathbf{x}) &\underset{M\to\infty}{=} \log\{2+\int_{-1}^{1}d\xi\frac{\xi^2}{2M^2}\left(h^{\star}-\beta^{\star}\frac{\psi(\mathbf{x})}{2}\right)^2+o\left(\frac{1}{M^2}\right)\}\\ &\underset{M\to\infty}{=} \log 2+\frac{1}{6M^2}\left(h^{\star}-\beta^{\star}\frac{\psi(\mathbf{x})}{2}\right)^2+o\left(\frac{1}{M^2}\right).\end{aligned}\tag{91}$$

Therefore,

$$\int_{\mathcal{D}}\mathbf{dx}\,\log Z_M^{\star}(\mathbf{x})\underset{M\to\infty}{=}|\mathcal{D}|\log 2+\frac{1}{2M^2}\left(h^{\star}X_{tot}-\beta^{\star}E\right)+o\left(\frac{1}{M^2}\right).\tag{92}$$

From (90) and (92), we finally obtain

$$\mathcal{S}_M^{pol}[p_M^{\star,E}]\underset{M\to\infty}{=}\log 2M+\frac{1}{2|\mathcal{D}|M^2}\left(\beta^{\star}E-h^{\star}X_{tot}\right)+o\left(\frac{1}{M^2}\right).\tag{93}$$

C.2 Maxima of the entropy over the set of critical macrostates $p_M^{\star,E}$.

Using equation (93), let us now determine which distributions among the critical distributions achieve the maximum of the macrostate entropy, when M is large. In the next paragraphs, we will work with the reduced entropy

$$D(\beta^{\star},h^{\star})\underset{\text{def}}{=}\lim_{M\to\infty}\{-2M^2|\mathcal{D}|\,\mathcal{S}_M^{pol}[p_M^{\star}]+\log 2M\}=\left(h^{\star}X_{tot}-\beta^{\star}E\right).\tag{94}$$

The minima of $D(\beta^{\star},h^{\star})$ are the maxima of the macrostate entropy.

Let us introduce the auxiliary functions

$$f(z) = \sum_{l\,odd} \frac{(1|\phi_{0l})^2 \kappa_{0l}^2}{(\kappa_{0l}^2 - z)}, \text{ together with } \mathcal{F} = \frac{f^2}{f'}. \tag{95}$$

f is defined on $\mathbb{R} - \{\kappa_{0(2l+1)}^2, l \in \mathbb{N}\}$. $\mathcal{F}$ is defined continuously over $\mathbb{R}$ by taking $\mathcal{F}(\kappa_{0l}) = (1|\phi_{0l})^2 \kappa_{0l}^2 = 16\pi/|\mathcal{D}|$ for every odd value of l. Those functions are sketched on Figure 7. Using f and $\mathcal{F}$, it is straightforward to relate $h^\star$ and $\beta^\star$ to E and X_{tot} for each kind of solutions.

For a solution from the continuum,

$$X_{tot} = \frac{h^\star}{3} f\left(\frac{-\beta^\star}{6}\right), \quad 2E = \frac{h^{\star 2}}{9} f'\left(\frac{-\beta^\star}{6}\right), \text{ and } X_{tot}^2 = 2E\mathcal{F}\left(\frac{-\beta^\star}{6}\right). \tag{96}$$

For a mixed solution,

$$X_{tot} = \frac{h^\star}{3} f\left(\kappa_{k_0 l_0}^2\right), \quad 2E = p_{k_0 l_0}^2 \kappa_{k_0 l_0}^2 + \frac{h^{\star 2}}{9} f'\left(\kappa_{k_0 l_0}^2\right), \text{ and } X_{tot}^2 \leq 2E\mathcal{F}\left(\kappa_{k_0 l_0}^2\right). \tag{97}$$

For an odd eigenmode,

$$X_{tot}^2 = 2E_0 \kappa_{0l_0}^2 (1|\phi_{0l_0})^2 = 2E_0 \mathcal{F}\left(\kappa_{0l_0}^2\right). \tag{98}$$

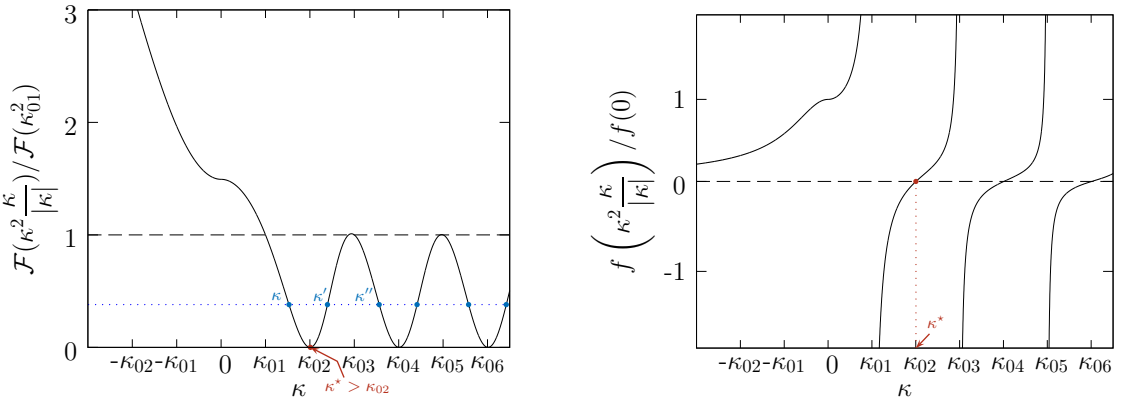

Figure 7: $\mathcal{F}$ and f as functions of κ. The minimum value $\kappa^\star$ for which both $\mathcal{F}$ and f are zero is greater than κ_{02}.

It is clear from Figure 7 and equations (96), (97) and (98) that we need to make a distinction between the cases $\frac{X_{tot}^2}{2E} > \mathcal{F}(\kappa_{01}^2)$, $\frac{X_{tot}^2}{2E} = \mathcal{F}(\kappa_{01}^2)$, and $\frac{X_{tot}^2}{2E} < \mathcal{F}(\kappa_{01}^2)$.

C.2.1 Case $\frac{X_{tot}^2}{2E} > \mathcal{F}(\kappa_{01}^2)$

In this case, there exists only one set of values for the Lagrange multipliers $(h^\star, \beta^\star)$ for which the constraints are satisfied. This set corresponds to a solution from the continuum. This solution is therefore the selected solution. As illustrated on Figure 7, there is a one to one correspondance between the value of $\beta^\star$ and the value of $\frac{X_{tot}^2}{2E}$. We can therefore write without ambiguity $\beta^\star = -6\mathcal{F}^{-1}\left(\frac{X_{tot}^2}{2E}\right)$.

If $\frac{X_{tot}^2}{2E} < \mathcal{F}(0)$, then $\beta^\star < 0$ and we define $\kappa(\beta^\star) = \sqrt{-\beta^\star/6}$. Otherwise, $\frac{X_{tot}^2}{2E} \geq \mathcal{F}(0)$, and $\beta^\star \geq 0$. We then define $\kappa(\beta^\star) = -\sqrt{\beta^\star/6}$. In both cases, $\kappa(\beta^\star) < \kappa_{01}$ and the other Lagrange multiplier is uniquely determined as $h^\star = \frac{3X_{tot}}{f\left(-\beta^\star/6\right)} = \frac{3X_{tot}}{f\left(\kappa^3/|\kappa|\right)}$.

C.2.2 Case $\frac{X_{tot}^2}{2E} < \mathcal{F}(\kappa_{01}^2)$

This case seems at first sight more intricated. First, there exist an infinite number of solutions from the continuum for which the constraints are satisfied. Indeed, for any odd value of l, there exist two values for the inverse temperature $\sqrt{-\beta^\star/6}$ in the interval $[\kappa_{0l}; [\kappa_{0l+2}[$ – denoted by κ and κ' on Figure 7. Second, there can exist an eigenvalue $\kappa_{k_0l_0}^2$ associated to an eigenmode $\phi_{k_0l_0}$ with $(1|\phi_{k_0l_0}) = 0$ such that $\mathcal{F}(\kappa_{k_0l_0}) > X_{tot}^2/2E$. In this case, there also exists a mixed solution associated to the eigenvalue $\kappa_{k_0l_0}^2$ for which the constraints are satisfied.

The situation is however easily settled because the following result holds true:

Result C.1 *Between two solutions that satisfy the same constraints, the one associated with the lower value of $|\beta^\star|$ has the lower reduced entropy – and hence achieves the higher macrostate entropy.*

From (C.1) we deduce that if $\kappa_{\min}$ denotes the smallest eigenvalue whose associated eigenfunction has a vanishing mean on the domain, then

- if $\mathcal{F}(\kappa_{\min}^2) \leq \frac{X_{tot}^2}{2E} < \mathcal{F}(\kappa_{01}^2)$, the selected solution is the solution from the continuum with inverse temperature $-6\beta^\star = \kappa^2 < \kappa_{\min}^2$ and $h^\star = 3X_{tot}/f(\kappa^2)$ uniquely determined from (96).
- if $\frac{X_{tot}^2}{2E} \leq \mathcal{F}(\kappa_{\min}^2)$, the selected solution is the mixed solution, with inverse temperature satisfying $-6\beta^\star = \kappa_{\min}^2$ and $h^\star = 3X_{tot}/f(\kappa_{\min}^2)$ uniquely determined from (97).

What remains to show is that (C.1) actually holds true. This is carried out in the next two paragraphs.

Maxima of the macrostate entropy achieved by solutions from the continuum. Let us first focus on solutions from the continuum. Those solutions are uniquely determined by the value of the inverse temperature $\beta^\star$. Indeed, from equation (96), given a value $\beta^\star$ such that $\mathcal{F}\left(-\beta^\star/6\right) = \frac{X_{tot}^2}{2E}$, $h^\star$ is uniquely determined as $h^\star = 3X_{tot}/f(-\beta^\star/6)$. Defining $\kappa(\beta^\star) = \sqrt{-\beta^\star/6}$, we can write the reduced entropy of such a continuum solution as

$$D^{(c)}(\kappa(\beta^\star)) = 6\kappa(\beta^\star)^2 E + \frac{3X_{tot}^2}{f\left(\kappa(\beta^\star)^2\right)}. \tag{99}$$

Let us now define

$$\kappa = \min\{\kappa' \,\big|\, \mathcal{F}\left(\kappa'^2\right) = \frac{X_{tot}^2}{2E}\}. \tag{100}$$

It is clear from Figure 7 that $\kappa \in [\kappa_{01}; \kappa^\star[$ where $\kappa^\star$ is the first zero of $\mathcal{F}$. Then, κ also achieves the minimal value of the reduced entropy (99), namely

$$D^c(\kappa) = \min\{D^c(\kappa') \Big| \mathcal{F}\left(\kappa'^2\right) = \frac{X_{tot}^2}{2E}\}. \tag{101}$$

Indeed, let $\kappa'' > \kappa$ such that $\mathcal{F}(\kappa''^2) = \mathcal{F}(\kappa^2) = \dfrac{X_{tot}^2}{2E}$.

- If $f(\kappa''^2) > 0$, then

$$D^{(c)}(\kappa) - D^{(c)}(\kappa'') = 6E\overbrace{\left(\kappa^2 - \kappa''^2\right)}^{<0} + 3X_{tot}^2\overbrace{\left(\frac{1}{f(\kappa^2)} - \frac{1}{f(\kappa''^2)}\right)}^{<0} < 0. \tag{102}$$

- Otherwise, let $\kappa' = \sup\{\kappa | \kappa < \kappa'' \text{ and } \mathcal{F}(\kappa^2) = \mathcal{F}(\kappa''^2)\}$. Then $f(\kappa'^2) > 0$ (see Figure 7), and

$$D^{(c)}(\kappa') - D^{(c)}(\kappa'') < 6E\left(\kappa'^2 - \kappa''^2\right) + 3X_{tot}^2 \frac{\kappa''^2 - \kappa'^2}{\mathcal{F}(\kappa'^2)} \leq 0. \tag{103}$$

The first inequality of equation (103) is obtained by using Tayor inequality at first order and by noticing that $(1/f)' = -1/\mathcal{F}$, while the second inequality stems froms the fact that $X_{tot}^2 = 2E\mathcal{F}(\kappa'^2) = 2E\mathcal{F}(\kappa''^2)$.

Hence,

$$D^{(c)}(\kappa) - D^{(c)}(\kappa'') = D^{(c)}(\kappa) - D^{(c)}(\kappa') + D^{(c)}(\kappa') - D^{(c)}(\kappa'') < 0. \tag{104}$$

Maxima of the macrostate entropy for continuum and mixed solutions. Let us now determine whether mixed solutions can achieve a higher macrostate entropy than solutions from the continuum. Consider for instance a mixed solution associated to the eigenvalue $\kappa_0^2 = \kappa_{k_0 l_0}^2$. Equation (97) tells that this solution exists provided $X_{tot}^2 \leq 2E\mathcal{F}(\kappa_0^2)$. Let us suppose this is the case. For this solution, the Lagrange multipliers are then uniquely determined as $\beta^\star = -6\kappa_0^2$, and $h^\star = \dfrac{3X_{tot}}{f(\kappa_0^2)}$. The corresponding reduced entropy reads

$$D^{(m)}(\kappa_0) = 6\kappa_0^2 E + 3\frac{X_{tot}^2}{f(\kappa_0^2)}. \tag{105}$$

We know from the preceding paragraph, that the minimum of $D^{(c)}(\kappa')$ is achieved for $\kappa \in [\kappa_{01}; \kappa_\star[$ uniquely determined. We therefore need to compare $D^{(c)}(\kappa)$ and $D^{(m)}(\kappa_0)$.

- If $\kappa_0 > \kappa_\star$, then inequalities similar to inequalities (102) and (103) yield $D^{(c)}(\kappa) < D^{(m)}(\kappa_0)$, so that the solution from the continuum has a lower reduced entropy and hence a higher macrostate entropy than the mixed solution.

- Otherwise, we need to have $\kappa_0 < \kappa < \kappa^\star$ in order for both solutions to exist. Then,

$$D^{(m)}(\kappa_0) - D^{(c)}(\kappa) \leq 6E\left(\kappa_0^2 - \kappa^2\right) + 3X_{tot}^2 \frac{\kappa^2 - \kappa_0^2}{\mathcal{F}(\kappa^2)} < 0, \tag{106}$$

and the mixed solution has a lower reduced entropy – and hence higher macrostate entropy – than any solution from the continuum that correspond to the same values of E and X_{tot}.

Similar inequalities show that when two mixed solutions can coexist, it is the one associated with the lower value of κ that also achieves the higher macrostate entropy.

This concludes the proof of (C.1).

C.2.3 Case $\frac{X_{tot}^2}{2E} = \mathcal{F}(\kappa_{01}^2)$

On this parabola, the only solutions that can exist are mixed solutions and pure odd mode solutions. For the odd eigenmodes, $h^\star = 0$, the reduced entropy simply reads $D^{(o)}(\kappa_{0l}) = 6E\kappa_{0l}^2$. It is then clear, that the eigenmode with the lowest value of $D^{(o)}$ is the gravest mode κ_{01}.

One can also notice that $D^{(c)}(\kappa_{01}+\epsilon) \underset{\epsilon\to 0}{\to} D^{(o)}(\kappa_{01})$. We can then extend by continuity inequality (106), so that if there also exists a mixed solution on the parabola $\frac{X_{tot}^2}{2E} = \mathcal{F}(\kappa_{01}^2)$, it is the gravest odd mode that solves the extremization problem.

C.2.4 Conclusion:

We can now conclude the discussion. Recall that $\kappa_{\min}$ denotes the smallest eigenvalue with vanishing mean on the domain. Note that $\kappa_{\min}$ is lower than the first zero of $\mathcal{F}$ (see Figure 7).

- For $X_{tot}^2 > 2E\mathcal{F}(\kappa_{01}^2)$, the selected solution is a solution from the continuum, with $\kappa < \kappa_{01}$ uniquely determined by E and X_{tot}.
- For $X_{tot}^2 = 2E\mathcal{F}(\kappa_{01}^2)$, the selected solution is the gravest eigenmode κ_{01}^2.
- For $2E\mathcal{F}(\kappa_{01}^2) > X_{tot}^2 \geq 2E\mathcal{F}(\kappa_{\min}^2)$, the selected solution is the one from the continuum associated to the value $\kappa_{01}^2 < \kappa^2 \leq \kappa^{\star 2}$.
- For $2E\mathcal{F}(\kappa_{\min}^2) \geq X_{tot}^2$ the selected solution is the mixed solution associated to the eigenvalue $\kappa_{\min}^2$.

D Computation of the critical points of the macrostrate entropy for the full problem.

We show how to compute the macrostate entropy (66) achieved by the critical distributions $p_M^\star$ (70) using the scaling (74). In addition to the reduced Lagrange multipliers defined in (74), we also define $\alpha_k^\star = \lim_{M\to\infty} M^2(\alpha_k^{(M)} - \alpha_k)$.

To derive the expression for the macrostate entropy, it is useful to express the Lagrange multipliers $h_k^\star$ and α_k in terms of the constraints. It is easily obtained from (67) and (70) that

$$A_k = |\mathcal{D}| \frac{\exp \alpha_k}{\sum_{k'=1}^K \exp \alpha_{k'}} \quad \text{and} \quad X_k = \frac{A_k h_k^\star}{3} - \frac{\beta A_k}{6\,|\mathcal{D}|} \int_{\mathcal{D}} \mathbf{dx}\, \psi\left(\mathbf{x}\right), \tag{107}$$

from which it follows that $\alpha_k = \log \frac{A_k}{|\mathcal{D}|}$ – up to an unphysical constant that can be absorbed in the partition function – and $\frac{X_{tot}}{|\mathcal{D}|} - \frac{X_k}{A_k} = \frac{1}{3}\left(\overline{h_k^\star} - h_k^\star\right)$.

The critical points of the macrostate entropy read

$$\begin{aligned}\mathcal{S}_M[p^\star_M] &= -\frac{1}{|\mathcal{D}|}\int_{\mathcal{D}}\mathbf{dx}\sum_{k=1}^{K}\int_{-M}^{M}\mathrm{d}\xi\, p^\star_{M,k}(\xi,\mathbf{x})\log p^\star_{M,k}(\xi,\mathbf{x}) \\ &= -\frac{1}{|\mathcal{D}|}\int_{\mathcal{D}}\mathbf{dx}\sum_{k=1}^{K}\int_{-M}^{M}d\xi\, p^\star_{M,k}(\xi,\mathbf{x})\left\{\alpha_k^{(M)}-\beta^{(M)}\frac{\sigma_k^2}{4y}\right. \\ &\qquad\left.+\left(h_k^{(M)}-\beta^{(M)}\frac{\psi(\mathbf{x})}{2}\right)\xi-\log M-\log Z^\star_M(\mathbf{x})\right\} \qquad (108) \\ &= \log M-\frac{1}{|\mathcal{D}|}\left(\sum_{k=1}^{K}\alpha_k^{(M)}A_k+\sum_{k=1}^{K}h_k^{(M)}X_k-\beta^{(M)}E\right)+\frac{1}{|\mathcal{D}|}\int_{\mathcal{D}}\log Z^\star_M(\mathbf{x})\,. \qquad (109)\end{aligned}$$

The last equality is obtained using $\int_{-M}^{M}\mathrm{d}\,\xi\, p^{\star,E}_M(\xi,\mathbf{x})=1$ on one hand, and using equation (67) to compute A_k, X_k, and E on the other hand. The asymptotic development of $Z^\star_M(\mathbf{x})$ for large M yields

$$Z^\star_M(\mathbf{x})\underset{M\to\infty}{=}2\sum_{k=1}^{K}e^{\alpha_k}\{1+\frac{1}{M^2}\left[\alpha_k^\star-\beta^\star\frac{\sigma_k^2}{4y}+\frac{1}{6}\left(h_k^\star-\beta^\star\frac{\psi(\mathbf{x})}{2}\right)^2\right]+o\left(\frac{1}{M^2}\right)\}. \qquad (110)$$

Hence,

$$\int_{\mathcal{D}}\mathbf{dx}\log Z^\star_M(\mathbf{x})\underset{M\to\infty}{=}|\mathcal{D}|\log 2+\frac{1}{M^2}\left\{|\mathcal{D}|\,\overline{\alpha_k^\star}-\beta^\star E^\star_{tor}+\frac{1}{2}\sum_{k=1}^{K}h_k^\star X_k\;-\frac{\beta^\star}{2}E_{pol}\right\}. \qquad (111)$$
$$+o\left(\frac{1}{M^2}\right)$$

From (111) and (109), we finally obtain

$$\mathcal{S}_M[p^\star_M]\underset{M\to\infty}{=}\log 2M-\sum_{k=1}^{K}\frac{A_k}{|\mathcal{D}|}\log\frac{A_k}{|\mathcal{D}|}+\frac{1}{2\,|\mathcal{D}|\,M^2}\left(\beta^\star E_{pol}-\sum_{k=1}^{K}h_k^\star X_k\right)+o\left(\frac{1}{M^2}\right), \qquad (112)$$

and equivalently the expression (79).

E Sanov theorem and entropy

Let us consider n independent and identically distributed random variables $\{s_k\}_{1\le k\le n}$ drawn with probability $f_0(s)\,\mathrm{d}s$. We consider the sum $S_n=\frac{1}{n}\sum_{k=1}^{n}s_k$ of these n variables and its distribution function

$$f_n(s)=\frac{1}{n}\sum_{k=1}^{n}\delta(s-s_k), \qquad (113)$$

Let us consider the probability distribution functionnal of ρ_n:

$$P_n[f]\equiv\langle\delta[f-f_n]\rangle\,, \qquad (114)$$

where the bracket is the average over the sampling of the variables $\{s_k\}_{1\le k\le K}$. Sanov theorem is a statement on the asymptotic behavior of $P_n[f]$. It states that

$$\log P_n[f]\underset{n\to\infty}{\sim}-n\int f\log\left(\frac{f}{f_0}\right)\mathrm{d}s, \qquad (115)$$

if $\int f\,\mathrm{d}s=1$ and $-\infty$ otherwise.

In the specific case when the variable s takes only K possible values $\{\sigma_k\}_{1\leq k\leq K}$ with probability $\{\pi_k\}_{1\leq k\leq K}$

$$f_0(s) = \sum_{k=1}^{K} \pi_k \delta(s - \sigma_k), \tag{116}$$

with $\sum_{k=1}^{K} \pi_k = 1$, then $f_n = \sum_{k=1}^{K} \rho_{k,n} \delta(z - \sigma_k)$.

We consider

$$P_n(\rho_1, ..., \rho_K) \equiv \langle \delta(\rho_{k,1} - \rho_1, ..., \rho_{K,1} - \rho_K) \rangle \tag{117}$$

the probability distribution function of $(\rho_{1,n}, ..., \rho_{K,n})$. Then Sanov theorem states that

$$\log P_n(\rho_1, ..., \rho_K) \underset{n\to\infty}{\sim} -n \sum_{k=1}^{K} \rho_k \log\left(\frac{\rho_k}{\pi_k}\right), \tag{118}$$

if $\sum_{k=1}^{K} \rho_k = 1$ and $-\infty$ otherwise.

We now consider a uniform network with N sites, as a discretization of a two dimensional surface of area $|\mathcal{D}|$. We denote by $\mathbf{r} = (x, y)$ points in this space. We consider a random s variable over this network. We assume that the values of s on each network point are uncorrelated among each other, and that at each point the variable can take one of the values $\{s_k\}_{1\leq k\leq K}$ with probability $1/K$. We can associate to this random variable s a set, an ensemble $C_N = [\![1; N]\!]^K$ of network realizations. The number of possible configurations, the cardinal of C_N is N^K. Through a coarse graining, we compute the local probability $\rho_k(\mathbf{r})$ to observe a value of s egual to σ_k in an infinitesimal area $\mathrm{d}\mathbf{r}$ around a point $\mathbf{r}$. We can apply Sanov theorem (118) to this case in order to compute $P_N(\rho_1(\mathbf{r}), ..., \rho_K(\mathbf{r}))$ to observe the values of s equal to σ_k in an infinitesimal area $\mathrm{d}\mathbf{r}$ around a point $\mathbf{r}$. Using $n = N\mathrm{d}\mathbf{r}/|\mathcal{D}|$ and $\pi_k = 1/K$, we get

$$\log P_N(\rho_1(\mathbf{r}), ..., \rho_K(\mathbf{r})) \underset{N\to\infty}{\sim} -\frac{N\mathrm{d}\mathbf{r}}{|\mathcal{D}|} \sum_{k=1}^{K} \rho_k \log(K\rho_k), \tag{119}$$

if $\sum_{k=1}^{K} \rho_k(\mathbf{r}) = 1$ and $-\infty$ otherwise. We can compute the probability $P_N[\rho_1, ..., \rho_K]$ to observe a field of local probabilities $(\rho_1(\mathbf{r}), ..., \rho_K(\mathbf{r}))$ over the whole space $\mathcal{D}$. Using that the values of s at different network locations are uncorrelated, we get

$$\log P_N[\rho_1, ..., \rho_K] \underset{N\to\infty}{\sim} -\frac{N}{|\mathcal{D}|} \sum_{k=1}^{K} \int_{\mathcal{D}} \rho_k \log(K\rho_k)\, \mathrm{d}\mathbf{r}, \tag{120}$$

if for all $\mathbf{r}$ $\sum_{k=1}^{K} \rho_k(\mathbf{r}) = 1$ and $-\infty$ otherwise.

With respect to the ensemble of network configurations, the functions $(\rho_1, ..., \rho_K)$ define a macrostate : all the realizations of the network that correspond to the local probabilities $(\rho_1(\mathbf{r}), ..., \rho_K(\mathbf{r}))$. We consider $\Omega_N[\rho_1, ..., \rho_K]$ the number of such microscopic configurations corresponding to this macrostate. We define as

$$S_N[\rho_1, ..., \rho_K] \equiv \frac{1}{N} \log \Omega_N[\rho_1, ..., \rho_K] \tag{121}$$

the specific entropy of this macrostate. This number of configuration is $\Omega_N = P_N N^K$ (using that the number of networks in the ensemble is N^K). From (119), using that $\sum_{k=1}^{K} \rho_k(\mathbf{r}) = 1$, we get

$$\mathcal{S}[\rho_1, ..., \rho_K] \equiv \lim_{N\to\infty} S_N[\rho_1, ..., \rho_K] = -\frac{1}{|\mathcal{D}|} \sum_{k=1}^{K} \int_{\mathcal{D}} \rho_k \log(\rho_k)\, \mathrm{d}\mathbf{r}, \tag{122}$$

for all $\mathbf{r}$ $\sum_{k=1}^{K} \rho_k(\mathbf{r}) = 1$ and $-\infty$ otherwise.

We now consider $C_N(A_1, ..., A_k)$ the ensemble of networks such that the number of σ_k on network sites is exactly $N_k = NA_k/|\mathcal{D}|$. This subset of C_N is exactly the ensemble used in order to define the microcanonical ensemble. A very classical combinatorial result gives that the cardinal is $\Omega_N(A_1, ..., A_k) \equiv \sharp C_N(A_1, ..., A_k) = N!/\Pi_{k=1}^K N_k!$. Using Stirling formula, we get that

$$S(A_{1,}...A_k) = \lim_{N\to\infty} \frac{1}{N}\Omega_N(A_1, ..., A_k) = -\sum_{k=1}^{K} \frac{A_k}{|\mathcal{D}|} \log\left(\frac{A_k}{|\mathcal{D}|}\right). \tag{123}$$

Let us show that we can get this result from the entropy result (122), thus avoiding combinatorial computations. The constraints $N_k = NA_k/|\mathcal{D}|$ are equivalent to

$$\int_{\mathcal{D}} \rho_k \, \mathrm{d}\mathbf{r} = A_k. \tag{124}$$

Then

$$S(A_{1,}...A_k) = \sup_{\{\rho | \int_{\mathcal{D}} \rho_k \, \mathrm{d}\mathbf{r} = A_k \text{ and } \sum_{k=1}^K \rho_k(\mathbf{r}) = 1\}} \{\mathcal{S}[\rho_1, ..., \rho_K]\}. \tag{125}$$

Using for instance Lagrange multipliers, it is easily proven that the supremum is reached for $\rho_k = A_k/|\mathcal{D}|$, from which we conclude once more the result (123). We can easily enforce other constraints. For instance the energy when it is meanfield like.

References

[Abarbanel et al., 1986] Abarbanel, H. D., Holm, D. D., Marsden, J. E., and Ratiu, T. S. (1986). Nonlinear stability analysis of stratified fluid equilibria. *Philosophical Transactions of the Royal Society of London. Series A, Mathematical and Physical Sciences*, 318(1543):349–409.

[Bouchet and Corvellec, 2010] Bouchet, F. and Corvellec, M. (2010). Invariant measures of the 2D Euler and Vlasov equations. *Journal of Statistical Mechanics: Theory and Experiment*, 2010:P08021.

[Bouchet and Venaille, 2011] Bouchet, F. and Venaille, A. (2011). Statistical mechanics of two-dimensional and geophysical flows. *Arxiv preprint arXiv:1110.6245*.

[Chavanis and Sommeria, 1998] Chavanis, P. and Sommeria, J. (1998). Classification of robust isolated vortices in two-dimensional hydrodynamics. *Journal of Fluid Mechanics*, 356:259–296.

[Ellis et al., 2004] Ellis, R., Jordan, R., Otto, P., and Turkington, B. (2004). A statistical approach to the asymptotic behavior of a class of generalized nonlinear Schrödinger equations. *Communications in mathematical physics*, 244(1):187–208.

[Ellis et al., 2000] Ellis, R. S., Haven, K., and Turkington, B. (2000). Large deviation principles and complete equivalence and nonequivalence results for pure and mixed ensembles. *Journal of Statistical Physics*, 101(5-6):999–1064.

[Eyink and Sreenivasan, 2006] Eyink, G. and Sreenivasan, K. (2006). Onsager and the theory of hydrodynamic turbulence. *Reviews of modern physics*, 78(1):87.

[Herbert et al., 2012] Herbert, E., Daviaud, F., Dubrulle, B., Nazarenko, S., and Naso, A. (2012). Dual local and non-local cascades in 3D turbulent Beltrami flows. *arXiv preprint arXiv:1206.5613*.

[Jordan and Turkington, 1997] Jordan, R. and Turkington, B. (1997). Ideal magnetofluid turbulence in two dimensions. *Journal of statistical physics*, 87(3):661–695.

[Kraichnan and Montgomery, 1980] Kraichnan, R. and Montgomery, D. (1980). Two-dimensional turbulence. *Reports on Progress in Physics*, 43:547.

[Leprovost et al., 2006] Leprovost, N., Dubrulle, B., and Chavanis, P. (2006). Dynamics and thermodynamics of axisymmetric flows: Theory. *Physical Review E*, 73(4):046308.

[Majda and Wang, 2006] Majda, A. and Wang, X. (2006). *Nonlinear dynamics and statistical theories for basic geophysical flows*. Cambridge University Press.

[Michel and Robert, 1994] Michel, J. and Robert, R. (1994). Statistical mechanical theory of the great red spot of Jupiter. *Journal of Statistical Physics*, 77(3):645–666.

[Miller, 1990] Miller, J. (1990). Statistical mechanics of Euler equations in two dimensions. *Physical review letters*, 65(17):2137–2140.

[Monchaux et al., 2006] Monchaux, R., Ravelet, F., Dubrulle, B., Chiffaudel, A., and Daviaud, F. (2006). Properties of steady states in turbulent axisymmetric flows. *Physical review letters*, 96(12):124502.

[Morrison, 1998] Morrison, P. (1998). Hamiltonian description of the ideal fluid. *Reviews of Modern Physics*, 70(2):467.

[Naso et al., 2010a] Naso, A., Monchaux, R., Chavanis, P., and Dubrulle, B. (2010a). Statistical mechanics of Beltrami flows in axisymmetric geometry: Theory reexamined. *Physical Review E*, 81(6):066318.

[Naso et al., 2010b] Naso, A., Thalabard, S., Collette, G., Chavanis, P.-H., and Dubrulle, B. (2010b). Statistical mechanics of Beltrami flows in axisymmetric geometry: equilibria and bifurcations. *Journal of Statistical Mechanics: Theory and Experiment*, 2010(06):P06019.

[Onsager, 1949] Onsager, L. (1949). Statistical hydrodynamics. *Il Nuovo Cimento (1943-1954)*, 6:279–287.

[Pomeau, 1994] Pomeau, Y. (1994). Statistical approach (to 2D turbulence). *NATO ASI SERIES B PHYSICS*, 341:117–117.

[Potters et al., 2013] Potters, M., Vaillant, T., and Bouchet, F. (2013). Sampling microcanonical measures of the 2D Euler equations through Creutz's algorithm: a phase transition from disorder to order when energy is increased. *Journal of Statistical Mechanics: Theory and Experiment*, 2013(02):P02017.

[Robert and Sommeria, 1991] Robert, R. and Sommeria, J. (1991). Statistical equilibrium states for two-dimensional flows. *J. Fluid Mech*, 229(29):l–3.

[Robert and Sommeria, 1992] Robert, R. and Sommeria, J. (1992). Relaxation towards a statistical equilibrium state in two-dimensional perfect fluid dynamics. *Physical review letters*, 69(19):2776–2779.

[Saint-Michel et al., 2013] Saint-Michel, B., Dubrulle, B., Ravelet, F., and Daviaud, F. (2013). Forcing-dependent stability of steady turbulent states. *arXiv preprint arXiv:1301.1810*.

[Szeri and Holmes, 1988] Szeri, A. and Holmes, P. (1988). Nonlinear stability of axisymmetric swirling flows. *Philosophical Transactions of the Royal Society of London. Series A, Mathematical and Physical Sciences*, pages 327–354.

[Thalabard, 2013] Thalabard, S. (2013). *Contributions to the statistical mechanics of quasi-2D flows*. PhD thesis, In preparation.

[Weichman, 2012] Weichman, P. B. (2012). Long-range correlations and coherent structures in magnetohydrodynamic equilibria. *Physical review letters*, 109(23):235002.